

Review

# Nanostructure Modified Electrodes for Electrochemical Detection of Contaminants of Emerging Concern

Taiwo Musa Adeniji and Keith J. Stine \* 

Department of Chemistry and Biochemistry, University of Missouri-St. Louis, St. Louis, MO 63121, USA

\* Correspondence: [kstine@umsl.edu](mailto:kstine@umsl.edu)

**Abstract:** We discuss the development of electrode surfaces modified with nanostructures for the electrochemical detection of contaminants of environmental concern (CECs) in the environment. The CECs are found in substances we all use in our daily lives such as pharmaceuticals, pesticides, flame retardants, personal care products, and so on. These contaminants pose a threat to human and environmental wellbeing, hence the need for effective methods for the fast and sensitive detection of these contaminants in our ecosystems. We describe the different electrochemical techniques researchers have used in the past for the detection of these pollutants in different environmental matrices. We survey the nanomaterials used to modify the electrodes used such as nanoparticles, nanowires, graphene, nanotubes and others used by researchers to detect these pollutants. The sensitivity of each approach is covered for numerous examples and nanomaterial-modified electrodes typically offer superior performance over more standard electrodes. We review the properties of these modifiers that make them good for the job and we looked at directions that researchers can pursue to further improve the sensitivity and selectivity of these modified electrodes.

**Keywords:** contaminants of emerging concerns; amperometry; voltammetry; electrode; nanoparticle; nanotube; graphene



**Citation:** Adeniji, T.M.; Stine, K.J. Nanostructure Modified Electrodes for Electrochemical Detection of Contaminants of Emerging Concern. *Coatings* **2023**, *13*, 381. <https://doi.org/10.3390/coatings13020381>

Academic Editor: Ioannis V. Yentekakis

Received: 23 December 2022

Revised: 1 February 2023

Accepted: 2 February 2023

Published: 7 February 2023



**Copyright:** © 2023 by the authors. Licensee MDPI, Basel, Switzerland. This article is an open access article distributed under the terms and conditions of the Creative Commons Attribution (CC BY) license (<https://creativecommons.org/licenses/by/4.0/>).

## 1. Introduction

In recent times, an increase in industrial and agricultural activities, urbanization, and mining activities, to name a few, has resulted in difficulty in waste management and disposal. The buildup of these wastes and the discharge of industrial and agricultural by-products like pesticides, UV-filters, drugs, and so on has led to the release of potentially dangerous and toxic compounds or substances into our ecosystems [1–3]. Some of these compounds are new to us; however, others have been used for a long time, and we just did not recognize them as hazardous. As a result, little or no regulations exist on the safe use and handling of these compounds and the full extent of their effect on the environment is not completely recognized [3]. These substances or compounds are known as contaminants of emerging concern or emerging pollutants, and in this review, they are referred to as CECs. Figure 1 is an image depicting various sources and transport of CECs within the environment [4].

Contaminants of emerging concern can thus be defined as pollutants that are not part of the established monitoring and evaluation programs and subject to the research done on the health risks they pose, ecotoxicity, and evaluation and monitoring data on their activities and occurrence in the ecosystem, they may be labelled a prospect for future regulations. CECs were also defined as chemical substances that may occur naturally or through human activities, which exist or are suspected to exist in different environmental matrices, ranging from soil, air, to water, with toxicities that could change the metabolic processes in living organisms [1]. Global attention has recently been drawn to the environmental fate of CECs like per- and polyfluoroalkyl substances (PFAS), micro- and nano plastics (MPs and NPs), additives (such as bisphenols/phthalates), flame retardants (FRs)

like polybrominated biphenyl diethers (PBDEs) and organophosphorus flame retardants (OPFRs), and nanoparticles. CECs have various applications in pesticides, pharmaceuticals, personal care products like sunscreens, nanomaterials, flame retardants, and so on [5]. Table 1 shows a list of CECs present in these compounds, their source, and effects on the ecosystem. Researchers are increasingly carrying out different studies on these pollutants, as much is not known about them, and this would help precisely detect their presence in the ecosystem, reduce these pollutants, and set an environmental quality standard for these pollutants.

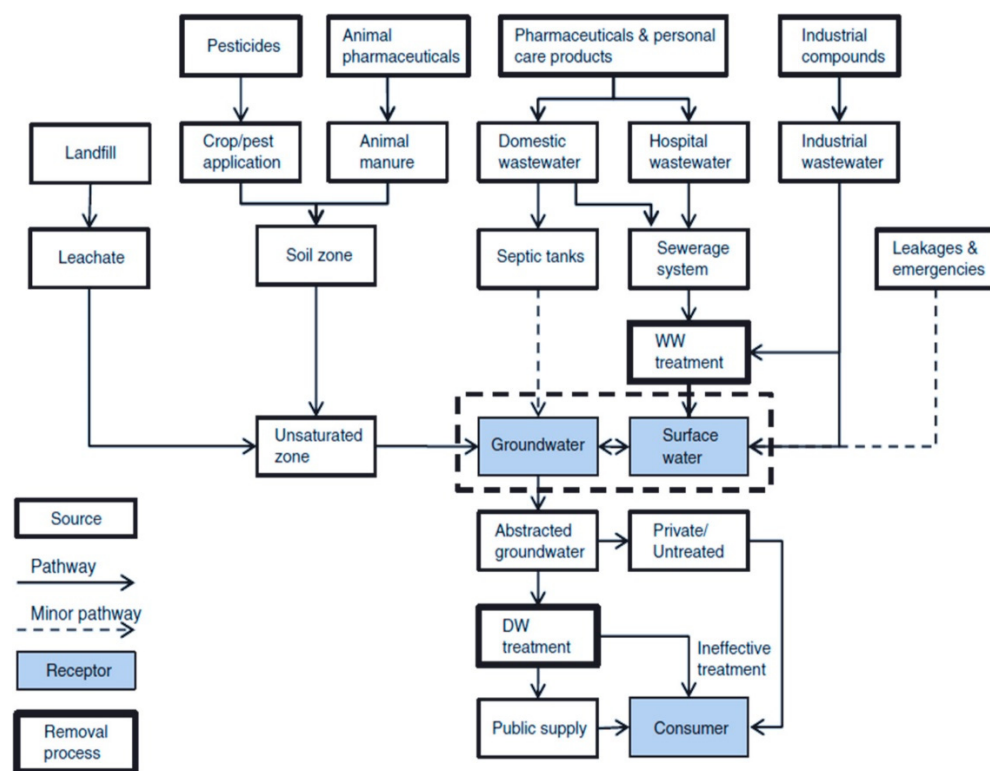


**Figure 1.** Scheme depicting various sources and transport of CECs from source to receptors. Reprinted with permission from [4]. Copyright 2019 American Chemical Society.

**Table 1.** CECs present in the ecosystem, their sources, and effects on the ecosystem.

| CECs/Sources   | Effects   | Ref. |
|--|---|------|
| 17-β-estradiol/Pharmaceuticals.                                  | Affects aquatic animal health negatively and is a major threat to aquatic ecosystems        | [3]  |
| Per- and polyfluoroalkyl/Coatings and water-resistant materials. | Severe endocrine disruption effects, potential carcinogen                                   | [4]  |
| Magnetite nanoparticle/Engineered NP                             | Exposed earthworms developed skin discoloration and intestinal disintegration at high doses | [6]  |
| CuO-NPs/Engineered Np  | Leads to stunted growth in plants   | [7]  |
| Acetaminophen(N-acetyl-p-aminophenol)/Pharmaceuticals            | Linked to a higher death rate; kidney, digestive, and cardiac disease                       | [3]  |
| Bisphenol-A/EDCs   | Decrease in fertility as well as problems with reproduction and growth                      | [8]  |

The detection of these pollutants in the environment is one of the major problems researchers are pursuing, as current detection tools and techniques involve considerable

sample collection and treatment, complex detection procedures that require trained laboratory personnel to carry out, as well as high cost of operation and lack of on-site detection tools for rapid testing [9]. In environmental and food analysis, a variety of analytical techniques are commonly used. Nuclear magnetic resonance (NMR), atomic spectroscopy (AS), gas chromatography (GC), capillary electrophoresis (CE), and solid phase extraction (SPE) are common examples, along with electrochemical detection. Analytical techniques such as inductively coupled plasma mass spectrometry (ICP-MS), hydride generation atomic absorption and emission spectrometry (HG-AAS/AES), atomic fluorescence spectrometry (AFS), and high-performance liquid chromatography have been widely reported for the determination of inorganic pollutants (HPLC) [10]. The use of GC for the analysis of CECs has been extensively applied and recently has evolved in directions of 2D GC [11] and coupled with mass spectrometry [12]. A variety of extraction techniques are available for preparing CEC samples for chromatographic analysis, including solid phase microextraction, liquid phase microextraction, and several other related methods [13]. It is necessary to account for the possible extraction of other components that may interfere with the analysis [14]. GC analysis of compounds from aqueous samples is dependent on their volatility [15]. Electrochemical methods can be directly applied to aqueous samples without need for solvent extraction and electrochemical instrumentation is less expensive and can be made portable [16]. Electrochemical detection methods are the most efficient, cost-effective, stable, sensitive, selective, and time-efficient of these techniques [17,18]. CECs detection methods based on electrochemistry are classified as voltammetric, amperometric, potentiometric, and impedimetric. Voltammetric methods like cyclic voltammetry, square wave voltammetry, and differential pulse voltammetry have advantages such as precision, simplicity, speed, selectivity, and cost-effectiveness [19].

An electrochemical sensor should have the ability to respond continuously and reversibly without disturbing the sample in order to provide accurate and timely information about a particular chemical composition in a specific environment [20]. Sensors typically consist of two main parts: a recognition element for selective/specific binding with the target analytes, and a transducer for transmitting information about that binding. Response time, signal to noise (S/N) ratio, selectivity, linear range, and limits of detection (LOD) are all aspects of recognition that depend largely on these two aspects of a sensor's performance [21]. Enhancing the sensor surface's conductivity to achieve high electron transfer between the analyte and biosensor surface is a major strategy used in the design of electrochemical sensors. To create electrochemical sensors, conductive components must be used [22]. Numerous modifications make it possible to detect pollutants selectively and sensitively since the working electrode is the most crucial component of an electrochemical sensor. It has been demonstrated that common working electrodes, ranging from carbon-based electrodes in various forms, such as carbon paste electrodes (CPE), glassy carbon electrodes (GCE), pencil graphite electrodes (PGE), screen-printed electrodes (SPE), to metallic solid electrodes like gold electrodes, are effective at sensing [23].

The poor surface kinetics of many conventional electrodes, which significantly impair the electrodes' selectivity and sensitivity, are known to cause a number of critical problems. On conventional electrodes, analytes often display a broad peak, and typically, no peak is present at lower concentrations [24]. Since the bare electrode surfaces interact with different types of materials and air, they are not particularly sensitive when used for trace level sensing straight from factory or lab storage. Pretreatment that specifically targets the electrode's surface shape and structure on a molecular basis can serve to clean and activate the electrode surface [10,24]. On the electrode surface, the material used to modify the surface can take the form of electroactive thin films, monolayers, or thicker coatings formed by methods such as drop-casting. Surface-modified electrode manufacturing is a cutting-edge technique for transforming conductive materials into functional electrodes suitable for biological settings [25]. The following phenomenon occurs when an electrode surface is modified: the physicochemical properties of the modifier are brought onto the

electrode and there is an increase in electrocatalytic activity, often because of an increase in surface area [23].

Through the years, several different techniques for modification have been investigated. Recent studies have shown that nanoparticle-modified electrodes can be very useful in electrochemical sensor technology if properly designed and constructed [9]. Gold is excellent for the fabrication of nanomaterials because gold nanoparticles (AuNPs) are great scaffolds for the development of cutting-edge chemical and biological sensors due to their unique physical and chemical properties. To begin, AuNPs may be easily produced and made to be very stable. Additionally, they have exceptional optoelectronic properties. Third, with the right ligands, they offer a high surface-to-volume ratio and great biocompatibility. To conclude, the size, shape, and chemical environment of AuNPs all have a significant impact on their attributes. Finally, AuNPs provide a versatile substrate for the attachment of a large variety of chemical or biological ligands, allowing for the selective binding and detection of small molecules and biological targets [21].

Metal–organic frameworks (MOFs) have recently been employed to modify electrodes for voltammetric measurement of inorganic and organic substances. As we will see in greater detail later in this review, the strong sorption capability of the MOFs towards the targeted analyte causes chemically modified electrodes to show increased accumulation of the analyte. As a result, there are numerous benefits to voltammetric analysis with such modified electrodes, including extraordinarily low detection limits, great selectivity, and the ability to determine multiple analytes simultaneously [26]. We will also be looking at the other types of modification methods in this review.

The focus of this review is to look at the different ways in which electrodes have been modified with nanostructures and nanomaterials for electrochemical sensing of emerging contaminants and outline the advances made towards achieving this goal. To do justice to the topic, we also must understand how effective bare electrodes are towards achieving sensing of these contaminants, and to do this, we will be mentioning different kinds of electrodes that are useful for electrochemical detection. It would also be important to mention the electrochemical techniques commonly used for the detection of these contaminants. A related book chapter [27] has focused on the advances in the use of nanostructures for the electrochemical and optical detection of the five active pharmaceutical compounds acetaminophen, folic acid,  $\alpha$ -lipoic acid, melatonin, and azathioprine whose detection has emphasized use of carbon-based nanostructures, metal oxide and metal nanoparticles. This paper covers both a range of nanomaterials that can be incorporated into these new electrochemical sensors and the wide range of analytes that are being pursued.

## 2. Contaminants of Emerging Concern Occurrence

Emerging contaminants are those that come from a new source, necessitating new methods of treatment and identification, and are categorized according to the degree to which they pose a threat to both the environment and human health. Wastewater from factories, farms, households, laboratories, and hospitals are all potential sources. In general, these contaminants can be traced back to one of three categories, namely, personal care products (PCPs), endocrine-disrupting compounds (EDCs), pharmaceuticals (PhACs), flame retardants (FRs), pesticides, artificial sweeteners (ASWs), and their metabolites [28,29]. We will be discussing other categories of CECs that exist as we advance in this review. Many of these compounds' existence in aquatic ecosystems and possible impacts on aquatic species and humans are poorly defined. Organic compounds are toxic to fish, animals, and potentially people. Many organizations like National Ocean and Atmospheric Administration (NOAA), the U.S. Geological Survey (USGS), and the U.S. Environmental Protection Agency (U.S. EPA) invest millions of dollars and great efforts to monitor trace quantities of organic compounds in surface waters, sediments, and aquatic creatures, which are not new substances but pose dangers to humans, aquatic, and terrestrial environments [30].

### 2.1. Water (Ground Water, Surface Water, Drinking Water, and Wastewater)

Despite the growing demand for safe and clean water, CEC regulation in drinking water is limited. The EU Council recently approved a proposal to update the Drinking Water Directive, which includes endocrine disruptors and pharmaceuticals for the first time. E2 and nonylphenol (NP) are on the watch list due to their endocrine-disrupting properties, while bisphenol A (BPA) is in the Directive [3]. Chemical pollutants can threaten potable water supplies if they make their way from the source of emission through layers of soil, riverbanks, aquifers, and other natural and manmade barriers. This transport can take a few days for surface water sources, a few weeks for riverbank filtration, or a few years for far-flung groundwater extraction wells. Important factors include the volume of emissions released into the environment and the substance's or its transformation products' persistence and mobility in aquatic ecosystems [31].

The advent of SARS-CoV-2 also contributed to an increase in the level of CECs in the environment. Kumari and Kumar, Achak and Khan noted that since hospitals generate a lot of wastewater from their kitchens, operating theaters, laundry rooms, and research labs, it stands to reason that they are also a major source of emerging contaminants and a major contributor to the high viral loads found in hospital wastewater. Emerging contaminants (such as pharmaceuticals and their transformation products) are released into the environment, not only through their patients' feces or urine, but also through the direct disposal of expired pharmaceuticals, cleaning agents, and disinfectants. Trace concentrations of these contaminants, which may range from  $\mu\text{g L}^{-1}$  to  $\text{ng L}^{-1}$ , pose a threat to public health and the environment if not properly treated and transported in wastewater or solids [32].

According to Vazquez-Tapia et al., 213 different CECs were detected in three different water matrices, including surface water, groundwater, and wastewater, according to an analysis of the 32 publications that were under review. Nevertheless, 174 of these contaminants were found, mostly in the  $\text{ng L}^{-1}$  range. A lack of monitoring programs and investigations regarding the occurrence, distribution, and environmental fate of these emerging contaminants in the Mexican water resources is indicated by the small number of scientific articles that have been published in the literature [8].

In a study carried out by Zhou et al., 477 substances belonging to 16 therapeutic groups were analyzed in European surface waters. Overall, 168 pharmaceuticals and 25 metabolites and transformation products were below the detection limits of the original analytical methods. The remaining 284 substances (243 pharmaceuticals and 41 metabolites and transformation products) detected at concentrations above detection limits belonged to 16 therapeutic groups: fungicides and antibiotics (73), analgesics and anti-inflammatories (30), anxiolytics and anticonvulsants (20), antihypertensives (19), antidepressants (19), opioids and morphine derivatives (18), stimulants (14), steroids and hormones (13), and antihistamines (9) (36). These groups were the most frequently detected in Europe and worldwide [33].

It is agreed that medicines enter the aquatic environment from wastewater sources, which are considered to be among the most significant point sources. There have been a great number of studies carried out in a variety of nations, including the United Kingdom, Australia, the United States of America, and Spain, which have reported that the wastewater contains anything from 16 to 54 different types of medications [34]. Every year, several manmade and natural chemicals are eaten and released into the environment. CECs are absorbed by the populace and accumulate in sewers, where they are only partially removed. The typical 60% removal rate of CECs in wastewater treatment systems is determined by treatment parameters, input loads, and the chemical's physicochemical characteristics and degradation resistance. Nonpolar molecules partition into sewage sludge, while water-soluble polar compounds remain in the aqueous phase. Inadequate WWTP retention time increases the risk that PFASs, stable benzotriazoles, and certain PPCPs may be discharged into the environment [35].

## 2.2. Aquatic Organisms

There has been a lot of focus on the potential ecological implications of CECs because their presence in water means constant exposure for aquatic animals. Therefore, it is thought to be important to study CECs in marine life. The presence of CECs in aquatic creatures may be indicative of CEC dispersion in the surrounding water environment, but it also suggests the potential for persistent pollutant transfer via the food web, which is dangerous for both human and environmental health [36].

In a study carried out by Deere et al., on the occurrence of contaminants of emerging concern in aquatic ecosystems utilized by Minnesota tribal communities, they discovered 117 CECs across 28 sites in northeastern Minnesota. Overall, 102 contaminants were detected in water, 67 were detected in sediments, and 35 were detected in fishes. Insect repellent (DEET) was found everywhere, with the highest quantities in underdeveloped areas. Endogenous hormones (e.g., estrone) and exogenous hormones, such as corticosteroids (e.g., hydrocortisone) and oral contraceptives (17 alpha-ethinyl-estradiol), were found in all sampling sites. All antidepressants examined were found in at least one medium. Antimicrobials, antineoplastics, and cardiovascular modifying drugs were detected at >35% [37].

Meador, Yeh, Young, and Gallagher carried out another study on the occurrence of CECs to determine the occurrence and concentrations of CECs in wastewater treatment plant effluent, estuary water, and two fish species (juvenile chinook salmon and staghorn sculpin) in the estuarine waters of Puget Sound receiving effluent, Washington, USA. They found out that in contrast to effluent and estuary water, fish were discovered to contain a number of chemicals that were not present in the former. Drugs like PFDA and PFOSA, as well as others like enalapril, benzotropine, fluocinonide, sulfadiazine, sulfamerazine, virginiamycin M1, and ormetoprim, fall under this category. Some of the fish released had likely been treated with ormetoprim, a drug commonly used in fish hatcheries and sold under the brand name Romet<sup>TM</sup>. Romet<sup>TM</sup> contains sulfadimethoxine, which was found exclusively in salmon, but was also found in effluent and estuary water. It is unclear whether the compound's presence in the fish's tissues resulted from exposure in the estuary or at the hatchery. They found a total of 42 chemicals in whole fish. CECs were found more frequently and at higher concentrations in juvenile Chinook salmon compared to staghorn sculpin [38].

## 2.3. Soil

Wastewater (WW) and biosolids can become contaminated with pharmaceuticals and other emerging contaminants (ECs), which could then be released into the environment. Wastewater treatment plants (WWTPs) in Canada, for instance, produce around 4 million tons of dry sludge annually. The high nutritional concentration of biosolids makes them a popular choice for soil enrichment in agricultural settings, public gardens, and greenhouses. Discharge from WWTPs has been shown to include high amounts of PPCPs and EDCs, indicating the existence of these substances in biosolids. As a result, municipal biosolids applied to land could initiate the bioaccumulation and magnify impact of ECs, upsetting the delicate equilibrium of biological systems from the cellular to the ecological [39]. A variety of entry points and transport mechanisms allow PFASs to reach the soil. PFASs from, say, firefighting foam find their way into landfills, wastewater treatment plants, and the atmosphere before settling out into the soil [40].

Shigei et al. evaluated the level of PFAS contamination in Jordan's Zarqa River (ZR), surrounding irrigated farms, soils, and vegetation. They observed that some amounts of PFASs from the Assamra WWTP have contaminated the Zarqa water used for irrigation and the soils in the fields of lettuce, mint, and alfalfa along the river. However, none of the plant material examined contained measurable amounts of PFASs, indicating that the crops under study are PFAS-safe for food [41].

#### 2.4. Atmosphere

Very little is known regarding the presence of other EC groups in the atmosphere, with the exception of polybrominated flame retardants, which have been researched in both indoor and outdoor settings. This paucity of knowledge must be taken into consideration because the breathing route cannot be ignored when determining the extent to which humans are exposed to these hazardous substances [42].

There are organic chemicals in the atmosphere, which interact with the oceans, the land, and all forms of life, including humans. It is not uncommon for particles in the air to be partitioned off into their own gaseous state. With a rise in molecular weight and a decrease in vapor pressure, the proportion of airborne particles increases. Therefore, CECs can be breathed, enter the respiratory system, and be deposited in the lungs, where they can attach to respirable air particles known as PM10 (Particulate Matter 10) or PM2.5. Research into a variety of respiratory disorders has found PM levels to be strongly correlated with death. The World Health Organization and the International Agency for Research on Cancer have both declared that there is sufficient evidence to classify outdoor air pollution as a human carcinogen, specifically a cause of lung cancer. Particulate Matters, a significant contributor to ambient air pollution, were subjected to independent assessment and were found to also be human carcinogen [43,44].

Two kinds of hydrophobic organic contaminants (HOCs), polycyclic aromatic hydrocarbons (PAHs) and organophosphorus esters, were investigated by Zeng et al. in collected fine and coarse PM from multiple probable emission sources in a megacity in South China (OPEs). Based on their research, organic and elemental carbon have a far greater influence on bioavailability in fine than in coarse particles. Bioavailability is more affected by organic carbon or elemental carbon than by particle size. Furthermore, the influence of carbonaceous materials depends on the physicochemical properties or emission sources of HOCs [44].

Another CEC that poses a great threat to human health are the microplastics. Microplastics pose a significant threat to ecosystems and human health because they are mobile, persistent, and easily ingested by species. Based on the results of the atmospheric microplastics analysis, synthetic textiles are the primary contributor to the presence of microplastics in the air. When washing and drying a garment, or any other fiber product, little fibers are readily torn out [45]. Until recently, not much research on microplastic suspension in air has been reported.

MPs were assessed in two private apartments and an office in Paris. Indoor air fiber concentrations ranged from 4.0 to 59.4 fibers/m<sup>3</sup>. The office has the most fibers per cubic meter (4.0–59.4), followed by apartment A (2.5–18.2) and apartment B (1.0–29.2) (1.1–16.3 fibers per m<sup>3</sup>). The fluctuation was due to MPs fiber emission from furniture and carpets due to repeated use and/or cleaning. Indoor MP levels were higher than outside in all three locations (0.3–1.5 fibers per m<sup>3</sup>). MPs were more diluted outside than inside, hence their origin was from within [46].

### 3. Classification of Contaminants of Emerging Concern

Contaminants of emerging concern (CECs) cover a wide range of substances, from pharmaceuticals (phACs) to personal care items to endocrine-disrupting compounds to flame retardants to pesticides to illegal drugs [28]. In this section, we discuss different classifications of CECs and compounds that fall under these classifications.

#### 3.1. Pharmaceuticals and Personal Care Products (PPCP)

Products that fall under the category of “pharmaceutical and personal care products” (PPCPs) include things such as toothpaste, skincare products, fragrances, antibiotics, and pharmaceutical medicines used for health and cosmetic purposes by consumers. Where conventional wastewater treatment plants fail to adequately remove PPCPs, their occurrence in our environment is on the rise. Emerging pollutants in aquatic and soil habitats may also be caused by waste from animal farms and sewage treatment plants [47].

Pharmaceutically active compounds (PhACs) can often be toxic. Pharmaceuticals are generally created from organic components (natural or synthetic) and used to cure and prevent disease and improve human and animal quality of life. Drugs make up a large portion of CECs, and their presence in drinking water raises worries about estrogenic and other deleterious consequences on people and wildlife. Three thousand substances, including impotence drugs, antidepressants, cholesterol regulators, contraceptives, beta blockers, anti-diabetics, antibiotics, and opioids, were deemed suitable as pharmaceutical solutions. As a result, it is a massive undertaking to establish rules, keep recommendations updated for all of these compounds, and monitor their spread throughout the environment; this is especially true when thousands more compounds are listed but not in regular use. Only a small number of these ECs have been examined in nature. Most over-the-counter drugs for pain and fever are nonsteroidal painkillers. Their manner of activation dictates how they behave throughout the body, and they have been detected in groundwater, typical streams, sediments, sludge, and WWTP effluents. They should boost the development of soil bacteria's anti-toxin defenses. These essentially unknown active pharmaceutical substances and their biotransformation components bio-accumulate and have a major impact on the biological system [19,28,48].

Pharmaceuticals and their metabolites entering the environment on a regular basis is an issue. Untreated sewage from residences, agricultural runoff into waterways, and aerial garbage disposal are a few examples of nonpoint sources. The sorptive capacity of solids (soils and sediments), the properties of the compounds' biotransformation, and the microorganisms present in treatment facilities all have an impact on the environmental contamination load. Environmental contamination is a result of flushing unneeded or expired pharmaceuticals down the toilet or down the sink drain [48]. Figure 2 is a pie chart that shows the patterns of consumption of various pharmaceuticals around the world [48]. Antibiotics are the most discussed medications due to their probable influence in bacterial resistance. Clarithromycin, azithromycin, and erythromycin are used in human, veterinary, and aquaculture medicine to prevent or cure pneumococci, staphylococci, and streptococci infections. These medicines were discovered in municipal WWTP effluents and other aquatic systems. Antibiotics have been found in wastewater, surface water, and groundwater in various nations at  $\text{ng L}^{-1}$  levels, with some investigations reporting several  $\text{g L}^{-1}$ . A Slovakia WWTP's effluents included  $\text{ng L}^{-1}$  of azithromycin, erythromycin, and clarithromycin [49]. The release of antibiotics from urban WWTP has been reviewed [50].

In reviews, fluorescence sensors, microbiological approaches, enzymatic quantification, spectrofluorometry, UV spectrophotometry, liquid chromatography linked to tandem mass spectrometry, and high-performance liquid chromatography have been used for quantitative drug assurance. These chromatographic techniques involve expensive equipment, well-trained personnel, lengthy cleaning, and long extractions. The methods use a lot of solvents, a considerable adjustment time, and variable enhancements such derivatizing treatment, flow rate, and mobile phase. Electroanalytical strategies can help solve these problems in the drug industry with a high level of affordability, selectivity, precision, and reliability based on consistent redox reactions at the electrode/solution interface. Electrochemical techniques have a high functional potential, high affectability and selectivity, reduced time, a basic pre-treatment strategy, and lower cost [22].

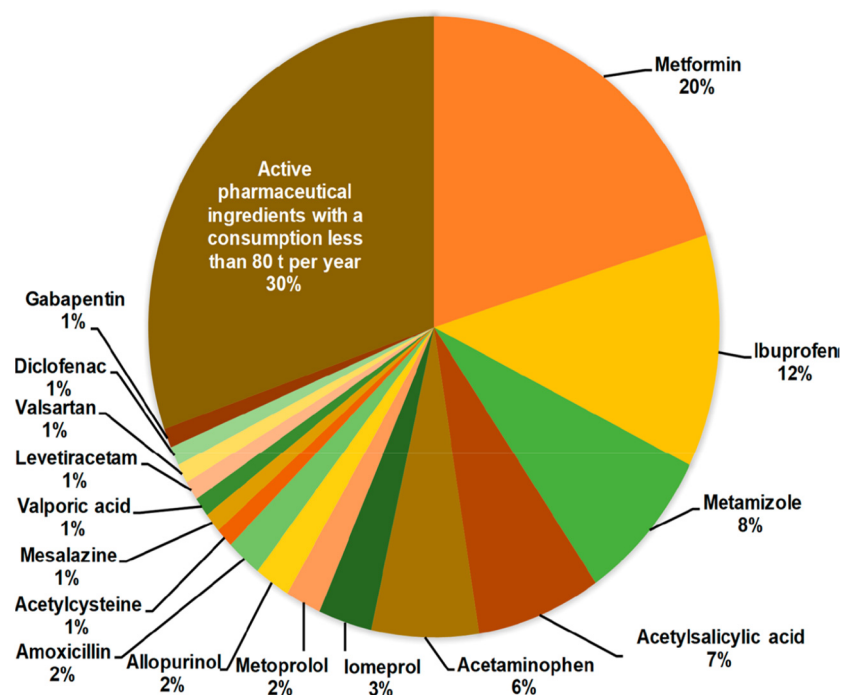


**Figure 2.** Pie chart showing the patterns of consumption of various pharmaceuticals around the world. Reprinted with permission from [50]. Copyright 2019, American Chemical Society.

### 3.2. Endocrine-Disrupting Compounds

One of the three primary information transmission systems found in humans is known as the endocrine system. It maintains an internal environment that is stable while also controlling a variety of physiological functions. Endocrine problems can cause illness. Chemicals that disturb normal endocrine function are referred to as endocrine-disrupting compounds (EDCs). These chemicals work by attaching to natural hormone receptors in order to change hormone production, storage, release, metabolism, and transport. EDCs are a recently discovered family of toxins that can be found in aquatic habitats and the effluents of industrial processes at very low concentrations [51–53].

Pollutants from a wide range of industrial chemicals can leak into the soil and groundwater, a feature shared by most urban and industrialized areas. Humans and other top-level predators are not immune to accumulating traces of these compounds as they move up the food chain. Exposure can occur through ingestion of polluted water, air, or food, or through skin contact with tainted soil. Workers in the pesticide, fungicide, and industrial chemical industries face a heightened risk of exposure and subsequent endocrine or reproductive problems [53]. Because of their ability to cause harm at extremely low concentrations (picomolar to nanomolar), EDCs pose a unique threat to developing organisms, including fetuses and infants; they have also been linked to higher rates of obesity, diabetes, infertility, and cancer. Since these molecules do not share a characteristic chemical structure, measurement is made more challenging. A portable, low-cost method of rapid and accurate detection of these compounds is therefore essential [54]. Electrochemical-based detection is a perfect solution to these challenges facing other analytical techniques.

One of many EDCs that have been administered as synthetic nonsteroidal estrogens with oral activity is diethylstilbestrol. According to a report, the substance may lower male human sperm counts [53]. In blood serum investigations carried out in the Netherlands, it was also shown that there was an association between reduced sperm counts and high quantities of polychlorinated biphenyl (PCB) [55]. Another study using rat tissue has reported on the transmission of EDCs to offspring. Other research may have determined further in-depth discussions on a range of areas of human health that were impacted by the exposure to EDCs [53].

In another research on the association of EDC exposure with earlier age of menopause, published by Grindler et al. in 2015, they discovered that at least one analysis linked nine PCBs, three pesticides, a furan, and two phthalates to earlier menopause. In at least one investigation, 14 of 15 EDCs demonstrated a dose–response association, suggesting that rising environmental exposures could alter ovarian function. These 15 substances cause menopause 1.9 to 3.8 years earlier than cigarette smoke, which causes it 0.8 to 1.4 years earlier. For each one unit rise in log EDC, the probabilities of menopause among 45–55-year-old women ranged from 1.3 to almost six-fold [56].

### 3.3. Pesticides and Agrochemicals

A pesticide is a chemical that eliminates unwanted organisms or prevents them from wreaking havoc in the natural world. Insecticides, plant pathogen killers, and microbial pesticides are all examples of common pesticides. Considering that pests and diseases are responsible for causing damage to up to one-third of crops, the use of pesticides plays a significant role in harvest quality and food protection, delivering great benefits to improve production. Massive worldwide use of pesticides and their breakdown products causes pollution of the environment and potential contamination of water supplies. Groundwater and surface water near large farms are at greater risk of contamination by pesticides, which is especially worrisome when considering their potential usage for human food. Numerous harmful effects, such as an increased incidence of cancer, birth deformities, genetic mutations, or other disorders like liver or central nervous system damage, attest to the impact of these toxins in the environment and to the wildlife. There is a lot of environmental concern about the presence of pesticides in water systems and the potential harm they could do to human health [57]. More than ninety-five percent of pesticides end up in unintended environments like air, water, and soil [47].

Due to the fact that the European Union has authorized the use of approximately 700 different types of pesticides, it is impossible to keep track of the presence of all compounds that are being applied as agrochemicals [2]. Aniline derivative, carbamate, chlorophenoxy compounds, organochlorine, organophosphate, pyridine, pyrimidine, triazine, and urea are key concerns. Some pesticides, including resmethrin, cypermethrin, bifenthrin, tolylfluanid, and methoxychlor, disrupt hormones by altering the glucocorticoid hormone receptor, a key endocrine factor. As a result, they may induce a variety of undesirable health effects [28]. Due to the inefficiency of WWTPs in removing pesticides, especially diazinon, diuron, atrazine, malathion, and simazine, the discharge from urban WWTPs is a primary reason for the release of pesticides into the aquatic environment [28]. Large amounts of pesticides are used for pest control due to the increased demand for food. The widespread use of pesticides and the toxicity of these chemicals poses a hazard to the environment, water, and food supply. Organophosphates, organochlorines, chlorophenols, carbamates, and synthetic pyrethroids are just some of the most widely used types of pesticides. The acute and chronic toxicity of these substances is mostly determined by the amount and length of time they are exposed to the substance [9].

### 3.4. Other Classes of CECs

Flame retardants (FRs) are chemicals added to combustible materials to stop or slow fires. These compounds save lives and reduce property damage. FRs fall into three chemical categories: (a) inorganic FRs, (b) halogenated (brominated and chlorinated) FRs, and (c) organophosphorus-containing FRs [58]. Organophosphate flame retardants (OPFRs), ATH, halogenated, and nitrogen-based flame retardants can lessen the flammability of numerous consumer and building products [59]. OPFRs are one of the most widely utilized FRs in furniture, textiles, construction materials, electronics, and processing chemicals. Floor polishes, coatings, engineered thermoplastics, and epoxy resins use OPFR plasticizers [58].

Nanotechnology and nanoparticles (NPs) have transformed science and technology. NPs' smaller size and high reactivity make them excellent for biological, pharmaceutical, electronics, defense, aerospace, and agriculture applications [60]. The majority of engi-

neered nanomaterials (ENMs) are released into the environment as pollutants during the various stages of production, product usage, recycling, and disposal (at an incinerator, landfill, or sewage treatment facility) [4].

Toxic heavy metals like Cu, Pb, Hg, and Cd in the soil, air, and water are absorbed by the structure of nanomaterials. These metals are hazardous and can lead to a number of diseases. Biological, chemical, and physical processes in the environment can cause ENMs to change their properties [48]. Invasion of nano-CuO disrupts normal physiological function and causes damage to intracellular and subcellular organelles. The accumulation of copper NPs in plant tissues may alter metabolic activities and cause the production of reactive oxygen species (ROS), which can damage DNA [7]. In the next section, various methods of modification of electrodes for sensing will be discussed.

#### 4. Electrode Materials Used for Electrochemical Sensing

##### 4.1. Glassy Carbon Electrode (GCE)

Glassy carbon is a term used to describe highly pure, non-graphitizing carbon that has undergone some coking during pyrolysis [61]. Studies have suggested that glass-like carbon, also known as glassy carbon or vitreous carbon, could combine the best qualities of both glass and ceramic with the strength and malleability of graphite. The most notable properties are extreme resilience to heat, low density, low electrical resistance, low friction, poor heat resistance, extreme resistance to chemical attacks, and complete impermeability to both liquid and gas [16]. As with defective fullerene-related nanoparticles, the microstructure of GC is made up of discontinuous fragments of curved carbon planes. A network of stacked ribbon molecules resembling graphite is seen in GC produced at high temperatures exceeding 2000 °C. GCs have a positive redox reaction to the analyte, quick and reversible electron transport without electrode fouling, a reasonably wide window of cathodic potentials at which the electrode can operate, an easily cleaned surface in between measurements, and no toxicity [62].

Over the years, GC has been the go-to electrode material in electrochemistry thanks to its low cost, superior electrical conductivity, electrochemical inertness over a wide potential window, wear resistance, chemical stability, impermeability, and easy surface modification [63]. Electrochemical tests can be taken at more negative potentials with GC as an electrode than with Pt or Au. Graphite electrodes, like GC, have a solid electrolyte interphase, although GC is more resistant to the deposition of lithium ions [62]. GCE is adaptable and can be used in a wide variety of sensing and detecting applications [64].

##### 4.2. Screen-Printed Electrode (SPE)

Due to its low cost, simple operation, and scalability, screen printing is a competitive technology for producing large quantities of printed microelectronics quickly. Inks are printed onto ceramic, plastic, or paper bases to create them [65]. Stencils, ink, and a squeeze blade are the standard components of screen-printing technology. Carbon's many benefits, including its chemical inertness, low background currents, and large potential window, have made SPEs a major focus as electrodes [66]. As can be seen in Figure 3, the entire electrode system in SPEs, including the reference, counter, and working electrodes, may be printed on a single substrate [67]. The glucose biosensor used to diagnose diabetes is a noteworthy example of a commercial application of screen-printed electrodes, and its global market is worth over a billion dollars annually [65]. Printing, drying, and curing are all essential phases in the manufacture of SPEs, and they have a major impact on the electrodes' ultimate electrochemical performance [68,69]. The sensitivity and selectivity of a SPE sensor are determined by a number of design considerations, including the ink's composition, curing temperature, pre-treatment procedures, and surface roughness [66].

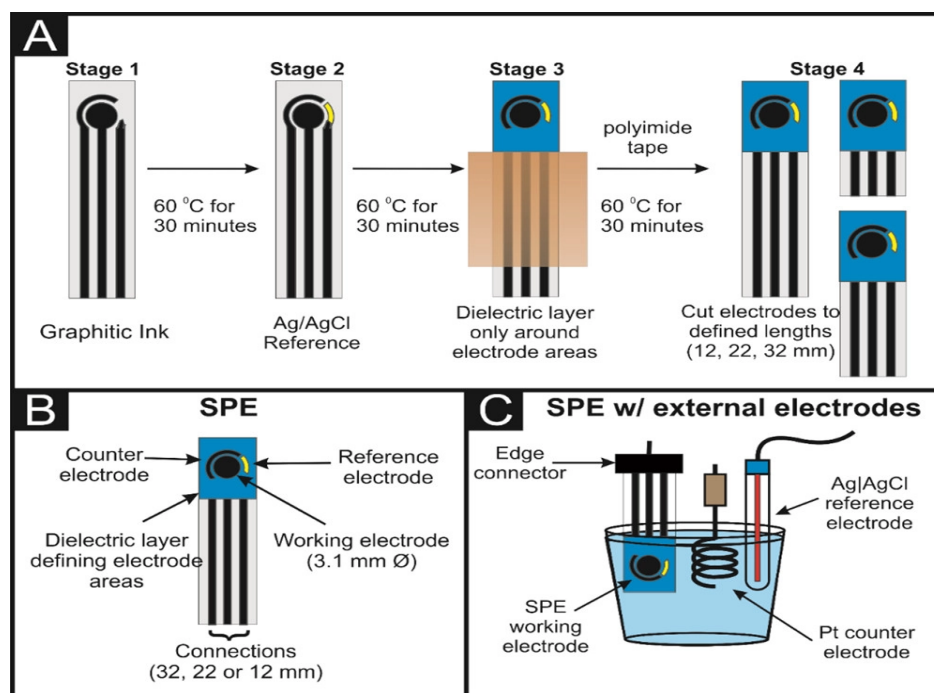


**Figure 3.** (A) Figure showing how to make SPEs using polyimide tape to reduce the amount of dielectric covering and make connection length adjustment simple. (B) A diagram depicting a SPE. (C) Three-electrode arrangement consisting of a SPE working electrode, Pt wire counter electrode, and Ag/AgCl reference electrode. Reprinted with permission from [67]. Copyright 2021, American Chemical Society.

#### 4.3. Gold Electrodes

Gold has a long history of being viewed as the ‘ugly duckling’ of the catalysis world due to the misconception that it is too noble to be effective as a catalyst. Although the catalytic activity of gold has been studied for centuries, it has recently come to the forefront of scientific inquiry in the last 30 years [70]. The previous 15 years, which have been described as a new gold “rush” age, have seen a remarkable increase in the use of gold and its nanostructures. Tradition holds that gold is a non-active metal when it is in its bulk form. However, the finding that gold nanostructures can serve as catalysts for heterogeneous reactions in both the liquid and gas phases led to the widespread use of gold in a variety of catalytic processes [71].

Gold’s suitability as a substrate for thiol conjugation chemistry, which permits the customization of surface functionality for various chemical and biosensing applications, has led to its widespread use in the sensing sector. Accurate sensor performance starts with the fabrication and characterization of gold or gold nanostructure-modified electrodes, which is essential in the development of reproducible and robust thiol conjugated surfaces [72]. When it comes to electrochemistry and electroanalysis, the most used metals for solid electrodes are gold and platinum. Reasons for this include the metals’ exceptional purity, their amenability to fabrication, and their “inertness” in the presence of nearly all chemicals. Platinum electrodes have historically been used for hydrogen reduction, even though gold has a higher overpotential. There were two main reasons given for this preference: tradition and the fact that gold is much harder to encapsulate in glass than platinum. Gold electrodes are becoming more popular due to two significant uses: stripping analysis and investigations involving surface modifications through self-assembly [73]. A typical three-way electrode electrochemical set up consists of a gold working electrode, on which several voltammetric techniques are carried out, a Ag/AgCl reference electrode, and a platinum counter electrode.

#### 4.4. Diamond-like Carbon Electrodes

To describe thin amorphous carbon films with physical and chemical properties akin to diamond, Aisenberg and Chabot coined the term “diamond-like carbon” (DLC). DLC is an amorphous carbon matrix that contains both sp<sup>3</sup>- and sp<sup>2</sup>-hybridized carbon, making it a metastable carbon allotrope [74]. Due to its corrosion resistance, wide potential window, and low background current, diamond-like carbon is a viable electrode material. Plasma-enhanced chemical vapor deposition (PECVD) at ambient temperatures produces hydrogenated amorphous carbon, a typical DLC [75]. DLC films are also used to protect optical windows, magnetic storage disks, vehicle parts, biological coatings, and micro-electromechanical systems [74]. In recent years, breakthroughs in the synthesis and purposeful adjustment of electrophysical properties, notably of carbon materials, allow them to be employed as electrodes in many electrochemistry applications. Finding an electrode material that is both corrosion-resistant and electrochemically active, with high electrocatalytic and stable working qualities, is a pressing task in the field of electrochemistry. Diamond and diamond-like material electrodes are ideal because they satisfy several of these criteria [76].

### 5. Electrochemical Sensing Techniques

Electrochemical detection methods are attractive due to their sensitivity, rapid response, and ease of use with relatively inexpensive equipment. Electrochemical sensors can be integrated into compact and portable devices for use in the field [77]. There are four major building blocks for electrochemical sensing systems: the transducer, the capture probe, the reporting probe, and the signal transduction technique. Working electrodes (WE), reference electrodes (RE), and counter electrodes (CE) make up the three-electrode setup used in electrochemical detection systems. Surface modifications to the WEs allow for their usage in the selective detection of distinct analytes.

In the development of an electrochemical sensor based on a working electrode surface modified with nanostructures the surface is typically first characterized with methods to determine the size, arrangement, and chemical structure of nanofeatures introduced such as nanoparticles, nanofibers, etc. Microscopy such as SEM and TEM are a key part in the characterization of the prepared modified electrode. The nanostructure may be studied as a composite prior to being drop-cast onto the electrode surface. Methods such as powder X-ray diffraction (PXRD), FTIR, and X-ray photoelectron spectroscopy can be used to confirm the structure and composition of nanomaterials used to modify the electrode surface.

Electrochemical methods can also be key to understanding the surface modification such as the use of electrochemical impedance spectroscopy (EIS) to evaluate the ease of electron transfer on the modified electrode surface. Electrochemical impedance spectroscopy is a technique that involves a plot of the impedance of a cell or electrode against frequency. Lock-in amplifiers and frequency response analyzers have largely replaced impedance bridges in modern laboratories because of their greater speed and convenience [78]. While nanomaterials can be deposited or formed directly onto an electrode surface, they are also often dispersed in a matrix of a polymer such as chitosan for better processing and stabilization. Faradaic EIS uses a soluble redox probe, most commonly Fe(CN)<sub>6</sub><sup>3−/4−</sup>, for its stability and simple one-electron reversible redox behavior. A small oscillation in potential (e.g., 5 mV) is applied and the frequency of the oscillation is incremented over a wide range (e.g., 10 μHz–5 MHz). The AC current response is used to determine the real and imaginary parts of the impedance which are then represented in a Zisman plot and fit to an equivalent circuit model. The most prominent parameter to emerge is R<sub>ct</sub>, and the charge transfer resistance is related to the diameter of a semi-circle like feature that appears in most Zisman plots. It has often been reported that modification of the electrode surface with the nanostructure(s) reduces the value of R<sub>ct</sub>, indicating that electron transfer to and from species in solution has been facilitated and made more efficient.

Amperometric and voltammetric methods are both useful. Amperometry is the practice of measuring current while the potential remains constant, while voltammetry

is the measurement of current while a controlled change in potential is occurring [79]. Electrochemical oxidation or reduction at the working electrode generates current, which is limited by the rate at which reactant molecules move from bulk solution to the electrode–solution interface. Benefits of voltammetry include accuracy, simplicity, speed, selectivity, and cost-effectiveness.

Characterizing and understanding the electrochemical behavior of the analyte can first be done using cyclic voltammetry (CV) to identify the positions and reversibility/irreversibility of observed oxidation and reduction peaks as a function of variables such pH and scan rate. The electrochemical behavior of the analyte on the unmodified and modified electrode surface should be compared. Differential pulse voltammetry (DPV) is the most popular method for detection of analyte and evaluation of sensor performance in terms of linear range, detection limit, and selectivity in the presence of potential interferents [80]. In DPV, the waveform applied is a series of pulses together with a staircase like pattern. The potential is held fixed for a period of time and the current is measured just prior to the application of a potential pulse of a specified height and duration. The current is measured again at the end of the pulse and the potential then decreases to a level that is a specified step above the initial level. The difference in the current after and before the pulse is plotted versus potential. The parameters of step height and duration, pulse height, pulse width, and pulse duration all need to be optimized. DPV reduces the contribution due to charging of the electric double layer and enhances the signal due to Faradaic processes. This is in contrast to CV, where larger background currents are observed. Square-wave voltammetry also reduces background currents and has a waveform consisting of a square wave superimposed on a staircase pattern. Voltammetric methods, including CV, DPV, SWV, and linear sweep voltammetry (LSV), have all been used in the development of electrochemical sensors [81]. The best detection sensitivities have been provided by DPV and SWV and these voltammetric methods are all distinguished by the characteristics of the applied potential waveform.

Amperometry involves monitoring the current as a function of time after injection of an aliquot of an analyte sample into electrolyte solution and recording the steady state current due to oxidation of the analyte on the electrode surface. Calibration plot of this current versus concentration can have an extended linear range and be used to establish the basis for sensor. Amperometric sensors can exhibit good selectivity and low detection limits [82]. Chronoamperometry is also used in experiments wherein the presence of analyte various interferents are added to see if they cause a change in the current response. Sensors typically consist of a recognition element that binds selectively and specifically to target analytes and a transducer component that transmits information related to the binding activity. When it comes to recognition, the reaction time, signal-to-noise ratio, selectivity, and detection limits of a sensor are determined by these two factors. Thus, the development of innovative modification methods to enhance the identification and transduction processes is crucial for the construction of more effective sensors [83]. The electronics of the instrument, the compatibility of the substrate, and the selectivity toward the analyte are all factors in determining which materials are most suited for sensing. High sensitivity can be achieved with the help of conductive substrates and a number of different surface modifications that both have binding sites for the analyte of interest and high conductivity.

## **6. Examples of Nanomaterials and Nanostructures Used in Electrochemical Sensors for CECs**

Nanomaterials have made it possible to miniaturize, transport, and create sensors with quick signal response times. Nanomaterials are very sensitive to changes in surface chemistry due to their high surface area to volume ratios and simple surface functionalization, which enables nanosensors to attain extremely low detection limits [84]. We now discuss the types of nanoparticles used for modification.

### 6.1. Nanoparticles of Metals and Metal Oxides

Nanoscale metallic materials have interesting catalytic and electrical properties. In order to achieve high specificity in a range of detection techniques, such as sensing pollutants, metallic nanoparticles are functionalized using several synthesizing methods [85]. There has been a lot of research into the use of metal nanoparticles (MNPs) and their oxides (MOX NPs) nanoparticle for chemical sensing because of their high reactivity and sensitive surface plasmon resonance. Due to their superior catalytic activity, conductivity, distinctive structure, and large specific surface area, metal nanoparticles such as gold, silver, platinum, palladium, copper, bimetallic, and others have been frequently employed to create electrochemical sensors with higher sensitivity.

Noble metal nanoparticles (NP) have been widely used in a range of sensor applications because of their ability to be generated in a wide variety of forms, their high extinction coefficients, and their easy surface functionalization [86]. There are a variety of sensing applications for metal nanoparticles. For instance, in sandwich-style assays, they can replace enzymes like horseradish peroxidase (HRP). In other applications, an analyte modulates metal nanoparticle activity, allowing a catalyzed reaction rate to be related to an analyte concentration.

### 6.2. Carbon Nanomaterials

Carbon-containing nanostructures stand out as a remarkable electrode material for improving the long-term stability of the electrochemical sensor, electro conductivity, and electro catalytic activity. As carbon nanomaterial-deployed electrochemical sensors often exhibit quicker electron transition kinetics than conventional detecting electrodes, lower limits of detection (LOD), and superior sensitivities, they are receiving increasing attention in research. Listed below are types of carbon nanomaterials.

#### 6.2.1. Graphene

For the first time, a single layer of graphene was successfully isolated from graphite by researchers at Manchester University led by Andre Geim in 2004 [87]. Graphene consists of a single layer of  $sp^2$  hybridized carbon atoms and has a hexagonal lattice structure in 2D. Because of its high carrier mobility and large specific surface area, graphene shows great promise as a material for use in electrical sensors [88]. Sensor devices can benefit from the superior mechanical, thermal, and electrical properties of graphene oxides (both exfoliated and reduced), as well as their large surface areas (up to  $2630 \text{ m}^2 \text{ g}^{-1}$ ).

#### 6.2.2. Carbon Nanotubes

Given their large surface area, high conductivity, and simplicity of functionalization, carbon nanotubes (CNTs) make an effective support structure. CNTs could further improve the efficiency of electrochemical analysis via immobilizing additional chemical species, such as organic molecules and metallic NPs [89]. High chemical stability, strong conductivity, and a large surface area explain why CNTs have attracted so much interest in the field of habitat rehabilitation. Stable electrochemical signal is achieved by multi-walled carbon nanotubes (MWCNTs) due to an increase in hydrophobicity at the interface, which negates the disruptive effect of the water layer.

### 6.3. Nanoporous Gold

Nanoporous gold (NPG) consists of interconnected bicontinuous structure of pores and ligaments in the typically several to tens of nanometers size ranges. Nanopores in NPG frameworks range in size from 20 to 50 nm, which could be as small as 5 nm [90]. In order to fabricate nanoporous gold (NPG), an alloy containing between 20 and 50 percent gold is typically leached selectively of less noble metal (s) like Ag. Because of its porous structure and network of ligaments, its surface area is disproportionately large compared to its volume. Due to its larger surface area, NPG can be utilized to boost the analytical signal from assays and hence increase their sensitivity. It has recently been reported that

NPG has been developed in array forms, which improves the potential for NPG to be used in screening technologies [91]. In particular, nanoporous gold (NPG) has been of interest for its potential in biological and analytical settings. Because of its numerous useful characteristics, including its large effective surface area, strong electrical conductivity, ease of surface modification using thiol-gold link chemistry, customizable pore size, and compatibility with traditional fabrication techniques, it has gained widespread attention. NPG has garnered attention as a promising material for a broad range of applications, including catalysis, energy storage, and the study of structure-property connections in the context of size-dependent mechanical characteristics. Applications of NPG in biomedical sciences have seen a recent uptick in attention, particularly because of the novel approaches it has taken to resolving long-standing problems in the areas of biosensing [92].

#### 6.4. Metal–Organic Frameworks (MOFs)

Metal–organic frameworks (MOFs) are a special kind of hybrid material with large and homogenous voids that exhibit unique features like an ordered crystalline structure, continuous porosity, high specific surface areas, outstanding thermal stability, and adaptable chemistry. There has been a surge in study of functional MOFs due to the breadth of interest generated by their potential uses in fields as disparate as gas storage, drug delivery, catalysis, optical imaging, and electrochemical sensors for selective sensing of various analytes [93]. Since MOFs may combine highly porous structures with a range of functional groups, they are particularly appealing as sensors because this allows analytes to quickly diffuse into their pores and promote framework-analyte interactions. One important component in synthesizing MOFs is the use of a metal center, and coordination around that center can result in modifications to the MOF's structure and characteristics. High-dimensional metal–organic frameworks (MOFs) were found to be easily prepared using transition metals with a higher coordination number or rare earth metals, and the prepared MOFs could serve as efficient electro-catalysts for small analytes. Multiple factors, including metal ions, organic linkers, ratio of reactants, type of solvent, pH, and supramolecular interactions (hydrogen bonding,  $\pi \cdot \cdot \pi$  stacking interactions), affect the final MOF structure during synthesis. Controlling and modulating structure typically requires the well-thought-out design of organic bridging ligands. Many metal–organic frameworks (MOFs) are poor choices for electronic components or electrodes because they lack conductivity. Adding guest molecules like iodine and tetracyanoquinodimethane TCNQ to facilitate charge transfer is one way to introduce electrical conductivity.

It is well-known that smaller particle sizes produce nanomaterials with larger surface areas, increasing the electroactive surface area. In addition, MOFs with hierarchically porous properties and distinctive structures, such as 2D MOF nanosheets and hybrid structures, will improve the accessibility of the electrode area and encourage the diffusion of analytes, improving the electron/mass transfer ability. Therefore, it has been demonstrated that creating nanoscale MOFs with distinctive architectures and hierarchical porosity characteristics is a practical way to further increase the sensitivity of sensors. In this review, we include examples of MOFs incorporating nanocomposite layers used to modify electrode surfaces.

Hydroquinone (HQ) and catechol (CT) were both found to be detectable in water samples when using a Cu-MOF-GN modified glassy carbon electrode, as reported by Li et al. [94]. In this research, a copper-centered metal–organic framework graphene composites (Cu-MOF-GN)-modified glassy carbon electrode (CuMOF-GN/GCE) was created for the simultaneous measurement of hydroquinone (HQ) and catechol (CT). The fabricated electrochemical sensor demonstrated outstanding performance in the detection of HQ and CT under optimum conditions, displaying a linear response in the range of 1.0  $\mu\text{M}$  to 1.0 mM with detection limits of  $5.9 \times 10^{-7}$  M for HQ and  $3.3 \times 10^{-7}$  M for CT ( $S/N = 3$ ), a broad linear range, good reproducibility, and long-term stability. This technique was successfully implemented for the direct determination of HQ and CT in municipal water supplies. Since

dihydroxybenzene isomers are important in electrochemical analysis, this work proposes a method for their determination.

## 7. Applications of Nanostructure-Modified Electrodes for CEC Detection

Electrode surface modification features a conductive substrate that has been modified with monolayers, electroactive thin films, nanomaterials, nanostructures, or thick coatings. Surface modifications can occur by processes such as electro-polymerization, self-assembly, ionic bonding, electrodeposition, drop-casting, or ionic hydride formation. Surface modifications are important for their effect on electrochemical interactions with the analyte during redox reactions. Furthermore, minor adjustments to the surface characteristics can determine the sensitivity of the measurements in electroanalytical applications. An attractive opportunity for the trace level identification of physiologically significant and environmentally harmful compounds with improved sensitivity and selectivity has been made possible by the modification of electrodes for use as sensors [23]. Electrode surface modification is a widely used method for enhancing the selectivity and sensitivity of electroanalytical detection by voltammetry. Electrodes are typically evaluated based on their limit of detection, which reflects their sensitivity and their ability to selectively identify the target in complex media [84]. The linear range of the response is also an essential feature.

We now discuss recent examples of different nanomaterial modifications of electrodes, how the detection with the modified electrodes was achieved and how effective these modifications are for the detection of CECs such as BPA, estrogens, pharmaceuticals, agrochemicals, and other types of CECs in the environment. Nanoparticles (NPs) of metals and metal oxides, MOFs, aptamers, polymeric materials, enzymes, and so on are all examples. Numerous modification procedures, including those involving synthetic metal ionophores, nanomaterials, and biological receptors like DNA or proteins, have been investigated throughout the years [9]. In subsequent sections, the different modification methods used in modifying electrodes will be discussed. Table 2 provides a summary of the nanostructures used to modify electrodes, the electrochemical sensing technique used in the detection of emerging contaminants, along with limit of detection and linear range(s) for the sensor summarized in this review.

### 7.1. Application to Detection of Bisphenol and Related Compounds

The organic molecule bisphenol A, also known as 2,2-bis (4-hydroxyphenyl) propane or BPA, is neither biodegradable nor chemically degradable, making BPA concentrations in the environment typically high. Numerous studies have demonstrated that BPA can mimic hormonal actions and interfere with such activities by interfering with growth, development, and reproduction; as a result, BPA has been classified as a significant endocrine disruptive compound (EDC) [95]. It is commonly utilized in water pipes, epoxy coatings on metal cans, food packaging materials, bottle caps, and plastics and resins. Food contamination with BPA has reportedly been found, depending on the food's kind and storage circumstances. As a result, the necessity of detecting various pollutants in food and environmental applications is rising steadily [96].

Extensive data suggest that 1–10 g mL<sup>-1</sup> of BPA is acutely harmful to freshwater and marine species of aquatic creatures and causes feminization of fishes, reptiles, and birds throughout their gonadal ontogeny [97]. Exposure to high levels of BPA in humans has been linked to a variety of health problems, including but not limited to diabetes, heart disease, breast and prostate cancer, infertility, and liver damage. BPA is also dangerous to aquatic ecosystems since it disrupts the development of many aquatic organisms. Because of its impact on human health, BPA has been restricted by governments all over the world. The use of BPA in polycarbonate baby bottles has been outlawed in a number of nations [98].

An early study of electrode development for bisphenol A detection made use of mesoporous silica MCM-41 mixed with graphite powder and paraffin oil made into a paste electrode [99]. Compared with related paste electrodes of MWCNT, activated carbon, silica gel, and graphite, the electrode including MCM-41 gave the superior response for a DPV

sweep in which bisphenol A was oxidized, presumably due to adsorption of bisphenol A into MCM-41 pores. An accumulation time of 3 min was used, and the optimal response was found at pH 8.0 and 20 wt.% of MCM-41 in the formulation of the paste electrode. The linear range was found to be 0.22–8.8  $\mu\text{M}$  and the detection limit was 0.038  $\mu\text{M}$ . Recovery from samples spiked into various local waters ranged from 91.3–107.3%.

MWCNT has proved useful for the construction of electrochemical sensors for bisphenol A [100]. A composite electrode on GCE was developed using MWCNT treated with nitric acid to introduce carboxylate groups. The treated MWCNT and Au NP were drop-cast on GCE in varying amounts for an optimization study. The DPV oxidation current on the optimally modified GCE was almost four times that seen on bare GCE. A linear range from 0.01–0.7  $\mu\text{M}$  was reported with a detection limit of 4.3 nM. Reproducibility over five prepared electrodes was 1.1% and over five repeated measurements was 1.5%. Recovery of sample spiked into river water and mineral water was 95.2–102.4%. A schematic of this approach and the DPV response is seen in Figure 4.

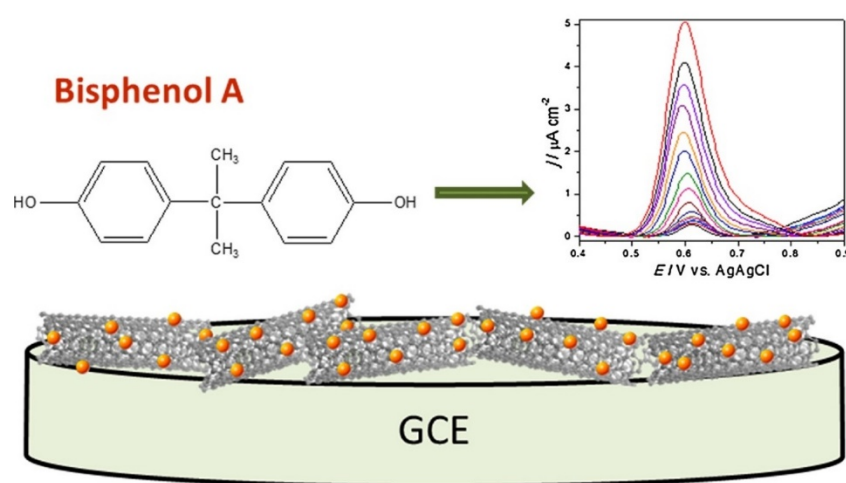


**Figure 4.** Depiction of Au nanoparticles decorated onto MWCNT oxidized to generate surface carboxylate groups and drop-cast onto GCE. Differential pulse voltammetry (DPV) was applied to detect bisphenol A. Reproduced from reference [100] with permission from Elsevier, copyright 2017.

Electrochemical sensors based on carbon nanomaterials, such as nanodiamond (boron-doped diamond) and nanocarbon, were designed by Jiang et al. to address the difficulties of monitoring trace amounts of BPA. They offered three methods: direct detection of BPA using boron-doped diamond on GCE electrodes, using disposable nanocarbon on GCE electrodes, and indirect detection of BPA using redox reaction of the by-product quinone on nanocarbon electrodes. The linear range for detection on nanodiamond/GCE was 0.1–50 mM and the detection limit was 5 nM as compared to a linear range from 0–30 mM and a detection limit of 0.5 mM on nanocarbon/GCE. A number of BPA sensors have been published in the literature, however the performance of these three approaches is superior. Recent medical advice has defined daily dose limitations for BPA, and the carbon-based sensors reported here can detect levels below them. These three sensors' key characteristic is the avoidance of surface fouling, the main issue for electrochemical BPA sensors, in addition to a lower detection limit and large detection range [101].

Niu et al. developed a practical electrochemical sensor for bisphenol A detection using stacked graphene nanofibers (SGNF) and gold nanoparticles (AuNPs) composite modified GCE. The AuNPs/SGNF modified electrode electrocatalyzed BPA oxidation, decreasing BPA oxidation overpotentials and increasing peak current compared to bare GCE and other modified electrodes. The transfer electron number ( $n$ ) and charge transfer coefficient ( $\alpha$ ) for BPA were  $n = 4$  and 0.52, indicating a four-electron and four-proton process for electrochemical oxidation on AuNPs/SGNF modified electrode. The effective surface area for the AuNPs/SGNF on GCE was 1.7-fold larger than bare GCE. The improved electrode's

kinetic characteristics showed an apparent heterogeneous electron transfer rate constant ( $k_s$ ) of  $0.51 \text{ s}^{-1}$ . Linear sweep voltammetry (LSV) was used to determine BPA and the linear range was found to be 0.08 to 250 nM with a detection limit of 35 nM. The modified electrode was used to detect BPA in baby bottles with good high sensitivity, long-term stability, and reproducibility [102].

To selectively detect BPA, Sanko et al. created a  $\text{Mo}_2\text{Ti}_2\text{AlC}_3$  and MWCNT composite. The synthesis and comprehensive characterization of transition metal carbide was performed using SEM and TEM. Based on the MAX phase material, the electrochemical sensor  $\text{Mo}_2\text{Ti}_2\text{AlC}_3$  exhibited improved electrical conductivity and electrocatalytic properties, enabling more selective and sensitive detection of BPA. Because it served as a suitable channel for electron transfer, the composite with MWCNT also had enhanced sensor qualities. The linear range of BPA concentrations observed was 0.01 to 8.5  $\mu\text{M}$ , with a limit of detection and a limit of quantitation (LOQ, 10 S/N) of 2.7 and 8.91 nM, respectively. In milk in plastic bottle and can samples, quantitative recoveries of 95.67–100.60% revealed sensitive detection of BPA at extremely low concentrations and with high selectivity with respect to other possible matrix chemicals [103]. Recently, copper ferrite nanoparticles have been combined with MWCNT to make a composite electrode by drop-casting a dispersion of these two components onto GCE [104]. The  $\text{CuFe}_2\text{O}_4$  nanoparticles in the composite were 47 nm in diameter on the 30 nm diameter MWCNT. A detection limit from DPV of 3.2 nM was found with a linear range from 0.01–120  $\mu\text{M}$ .

In order to achieve sensitive and selective measurement of BPA, Zhang et al. created a novel dual-signal sensor by connecting nanoporous gold leaf (NPGL) with thiolated beta-cyclodextrin (SH- $\beta$ -CD) [105]. Electrochemical measurements, scanning electron microscopy, and energy-dispersive spectroscopy (EDS) were all used to follow the course of NPGL modification and self-assembly of SH- $\beta$ -CD on gold electrode. In the dual signaling approach, signals from the target molecule BPA and the probe molecule methylene blue were simultaneously recorded in order to model the competitive host–guest interaction (MB). Since the host molecule ( $\beta$ -CD) binds to BPA differently than it binds to MB, the former can enter the latter's cavities, lowering the latter's oxidation peak current while increasing its own. A linear relationship was found between the total change in current and the logarithm of BPA concentration between  $3 \times 10^{-7}$  and  $1 \times 10^{-4}$  M, with a detection limit of  $6 \times 10^{-8}$  M. In contrast to employing just DIBPA as the response signal, the detection limit reached by dual-signaling was significantly lower. The sensor was also used to evaluate BPA in milk and municipal water supplies.

The best possible substitute for bisphenol A, bisphenol S, has been shown to be hazardous to humans. Unfortunately, no quick detection method has been developed to serve the on-site measurement of bisphenol S. In order to address this gap, Zhu et al. developed a novel electrochemical platform based on the co-reduction of graphene oxide and  $\text{C}_{60}$  nanoassembly cast onto GCE. The innovative electroanalytical platform enabled sensitive determination of bisphenol S by DPV in the range of 1–100  $\mu\text{M}$  with a detection limit of 0.5  $\mu\text{M}$ . The nanoassembly was generated by grinding. High electrocatalytic activity towards bisphenol S was found. This sensor was also used to identify bisphenol S in milk, with promising results for its anti-interference capacity and respectable recovery [106].

A peptide specific for binding to bisphenol A was developed as a recombinant LacI protein with the heptapeptide specific to bisphenol A (CKSLENSYC) inserted at the C-terminus end. Layer by layer assembly of the recombinant protein and reduced graphene oxide nanosheets onto quartz substrate. Denaturation of the recombinant protein yielded hydrophobic interactions necessary to immobilize the peptide sequence. The rGO thin film was 2 bilayers of rGO and 4 nm thick. EIS was used as the detection method and the increase in  $R_{ct}$  was linear from  $10^{-13}$  M to  $10^{-8}$  M BPA with a detection limit of 5.0 fM [107].

The polysaccharide chitosan has also proved useful as a component for the construction of nanocomposite electrodes that included also carbon nanotubes [108]. Chitosan cross-linked by glutaraldehyde was combined with carbon nanotubes and  $\text{TiO}_2$  nanoparticles in mineral oil to make a paste for the formation of an electrode referred to as a

carbon nanotube paste electrode. It was found that 10% TiO<sub>2</sub> nanoparticles were optimal. The linear range in DPV for the oxidation of bisphenol A was from 0.01–6.0 μM and the detection limit was 9.58 nM.

The orientation of single-walled carbon nanotubes (SWCNT) on an electrode surface was found to have a dramatic effect on the limit of detection for bisphenol A [109]. SWCNT wrapped by a special ssDNA with a terminal thiol are found to orient vertically relative to a gold electrode surface. Remarkably, the DPV detection limits for detection of oxidation of bisphenol A were 102.3, 45.8, and 11.0 nM for bare Au, Au covered by dispersed non-oriented SWCNT, and the vertically oriented SWCNT, respectively. The linear range for detection using the oriented SWCNTs was 0.5–3.8 μM. The sensitivity reported was 0.49 μA μM<sup>-1</sup> for oriented SWCNT on Au electrode and 0.24 μA μM<sup>-1</sup> for dispersed SWCNT on Au electrode. In another study, the effect of type of carbon nanotube on detection of bisphenol A was evaluated [110]. MWCNT of diameter 110–170 nm and those of diameter 20–40 nm was compared. The effect of acid treatment with HNO<sub>3</sub>/H<sub>2</sub>SO<sub>4</sub> (3:1 by volume) was also evaluated. The limit of detection and sensitivity was the best for the smaller diameter MWCNT that were acid-treated, 0.084 μM vs. 0.61 μM for the acid-treated larger diameter MWCNT. A GCE electrode modified with acid-treated MWCNT was reported to be able to electrochemically distinguish bisphenol AF from bisphenol F [111].

Mo et al. developed an electrochemical sensor for bisphenol A using AuPd incorporated onto polymer-wrapped carboxylic multi-walled carbon nanotube [112]. Poly (diallyldimethylammonium chloride) was first allowed to assemble around MWCNT in solution followed by citrate reduction of HAuCl<sub>4</sub> and PdCl<sub>2</sub> to create AuPd nanoparticles that could assemble onto the polymer-wrapped MWCNTs. Bisphenol A was found to be best accumulated on the electrode for a time of 50 s at -0.2 V (vs. SCE). DPV was used to detect bisphenol A using the oxidation peak near 0.5 V (vs. SCE). The linear range was 0.18–18.0 μM and the limit of detection was 60 nM. Bisphenol A detection was possible when spiked in either milk or in tap water with excellent recovery.

### 7.2. Application to Detection of Estrogen-like CECs in the Environment

An ever-increasing number of people these days are eager to find ways to stop the hands of time and restore their youth. Estrogens added to cosmetics have the potential to lighten skin, improve skin suppleness, get rid of wrinkles, and slow the aging process. Use of these drugs for an extended period of time, however, has been linked to an array of health problems, including endocrine disruption and several forms of cancer (including endometrial carcinoma, cell carcinoma, breast, and ovarian cancer). The three essential steroid estrogens, estradiol, estrone, and estriol, are significant bioactive compounds that play a role in intracellular communications and affect the emergence and upkeep of sex characteristics [113].

When introduced into an organism, phenolic estrogens disrupt the endocrine system, leading to aberrant reproductive or immunological functioning, hermaphroditism, sexual instability, reproductive organ impairment, and so on. Hexestrol (HEX), diethylstilbestrol (DES), dienestrol (DE), and bisphenol A (BPA) are the most widely used phenolic estrogens (BPA) [114]. Estriol was used for the treatment and prevention of hormonal imbalance-related problems, including cardiovascular disease, cancer, hyperandrogenism, osteoporosis, and urogenital diseases in females. Because it is eliminated in the urine and is not destroyed during sewage treatment, it is also considered an endocrine disruptor that is harmful to human and animal health [115].

An electrochemical immunoassay using DPV was developed for HEX, DES, DE, and BPA by Pan et al. Au nanoparticles (20–80 nm by SEM) were formed by electrodeposition on GCE and then modified by aminoethanethiol to which HEX was conjugated using EDC/NHS coupling. The introduction of monoclonal antibodies and phenolic estrogen results in a change in the DPV peak current near 0.2 V (vs. Ag/AgCl) for the redox probe Fe(CN)<sub>6</sub><sup>3-/4-</sup>. Detection limits of 0.25, 0.25, 0.15, and 0.20 ng mL<sup>-1</sup> were found for HEX, DES, DE, and BPA, respectively and the linear range of response vs. log(concentration)

extended up to 200, 2000, 500, and 500 ng mL<sup>-1</sup>, respectively. Recovery was excellent from samples spiked into supernatant extracts from beef, pork, and milk powder samples [116].

Raymundo-Pereira et al. detailed the electrochemical detection of estriol employing carbon black nanoballs (CNB) decorated with silver nanoparticles (AgNP) formed by the reduction of AgNO<sub>3</sub> from solution and drop-cast onto GCE [117]. Uniform, porous films were produced with CNB with widths of 20–25 nm and AgNPs of 5–6 nm in width. Cyclic voltammetry and electrochemical impedance spectroscopy showed that CNB/AgNP electrodes were more effective than bare GCE and GCE/CNB in terms of electron transfer and electroactive area. Estriol was detected using DPV in 0.1 M PBS (pH 7.0) with a linear range of 0.2 to 3.0 μM and a limit of detection of 0.16 μM. In a stream water sample, the sensor detected estriol with the same sensitivity as the gold standard approach based on HPLC.

An electrochemical sensor for the simultaneous detection of diethylstilbestrol (DES) and 17-β-estradiol (E2) in skin care toner was developed by Chen et al. using Fe<sub>3</sub>O<sub>4</sub>-doped nanoporous carbon (Fe<sub>3</sub>O<sub>4</sub>-NC), which was manufactured by carbonizing Fe porous coordination polymer (Fe-PCP), also known as metal–organic framework (MOF). Since estrogens frequently interact in natural samples, the ability to precisely quantify them is of paramount practical importance [118]. By using electro-catalytic oxidation at a Fe<sub>3</sub>O<sub>4</sub>-NC modified GCE (Fe<sub>3</sub>O<sub>4</sub>-NC/GCE), the levels of two common estrogens, DES and E2, were simultaneously determined. The detection limits for DES and E2 were 4.6 and 4.9 nM, respectively, and the DPV peak currents rose linearly as the concentrations increased from 0.01 to 12 μM and from 0.01 to 20 μM, respectively. The goal of this research was to analyze toner for both estrogens at once. The DES and E2 recoveries in real toner samples ranged from 91.2% to 110.4%. The experiments show that DES and E2 can be detected together in a real toner sample by using a sensor with superior anti-interference capacity.

Graphene nanoribbons (GNR) are a material prepared by ‘unzipping’ MWCNT under oxidizing conditions. A nanocomposite electrode was prepared by combining GNR with fumed silica that was decorated by Au nanoparticles modified by cysteamine and then drop-casting it over a carbon paste electrode (CPE) [119]. The fumed silica served to enhance surface area, Au NP, and GNR to increase conductivity and cysteamine to promote hydrogen-bonding. Raman spectroscopy was used to confirm the vibrational features of GNR. Using DPV, the sensor, when applied to detecting 17-β-estradiol, gave a linear range of 0.1–5.0 μM and a detection limit of 7.4 nM. The detection of 17-β-estradiol spiked into milk was successful.

17-β-Estradiol was also successfully detected using GCE modified by MWCNT that had been acid treated to produce polar and hydrophilic functional groups on the nanotube surfaces. The modified MWCNT were drop-cast onto GCE followed by drop-casting of Au NP of 20–30 nm diameter, the same as the average diameter of the nanotubes. Using linear sweep voltammetry, the optimal response was found at pH 7.0. A linear range from 1.0–20.0 μM was found with a detection limit of 70 nM. The sensor retained 79% of its initial response after 5 days. Recovery from samples spiked into wastewater, treated water, or tap water ranged from 94.7–98.5% [120].

Aptamers have also been employed as highly specific binding agents for 17-β-estradiol as part of a nanostructured electrode. Boron-doped diamond thin films were first formed by chemical vapor deposition onto p-Si(100) which was then treated with aqua regia to yield an –OH terminated surface. Using the hydrogen bubble template method, Zn nanoparticles were formed on the surface. The Zn nanoparticles served as templates for the electrodeposition of Au nanostructures in the form of tree-like dendrites. The gold surfaces were then modified at ssDNA 76-mer aptamer that was thiolated on one terminal end. The increase in charge transfer resistance upon binding of 17-β-estradiol to the aptamer was linear vs log([17-β-estradiol]) over the range 10<sup>-14</sup>–10<sup>-9</sup> M. A remarkably low detection limit of 5 × 10<sup>-15</sup> (5.0 fM) was found [121].

Javaid et al. described the electrochemical detection of methylparaben using a GCE modified with zinc oxide nanoparticles [122]. The chemicals in parabens have both estro-

genic and antiandrogenic properties. As was already established, these molecules have been linked to male infertility and cancers, including breast tumors. As a result, parabens are being considered as a possible health danger. The usage of medicinal items and cosmetics are the main ways that people are exposed to parabens. The ZnO nanoparticles were prepared using a sol-gel method and then mixed with carbon black and Nafion to prepare a paste that was drop-cast onto GCE. The ZnO nanoparticles were prepared as nanospheres (at pH 12), nanocuboids (at pH 10), and nanowires (at pH 8). ZnO nanowires performed best with a linear range from 0.02–12 mM and a detection limit of 7.25  $\mu\text{M}$ . Figure 5 shows the nature of these three different incorporated nanostructures and example CV curves. Each of the three ZnO samples was tested for its sensitivity to the electro-oxidation of methylparaben, and the results were compared in order to establish the impact of shape on sensing performance. The sensitivities from SWV were found to be 0.871, 0.151, and 0.134  $\mu\text{A mM}^{-1}$  for the GCE/ZnO nanowires, GCE/ZnO nanocubes and GCE/ZnO nanospheres, respectively. In comparison to the existing literature, which made use of sophisticated, costly, and multi-component materials, the nanowire (GCE/ZA8)-modified sensor demonstrated great selectivity towards MePa, high stability for a long length of time, and an acceptable LOD. The proposed sensor not only offers innovative detection of MePa using ZnO NPs, but also paves the way toward using simple non-precious metal systems for the electrochemical detection of water contaminants.

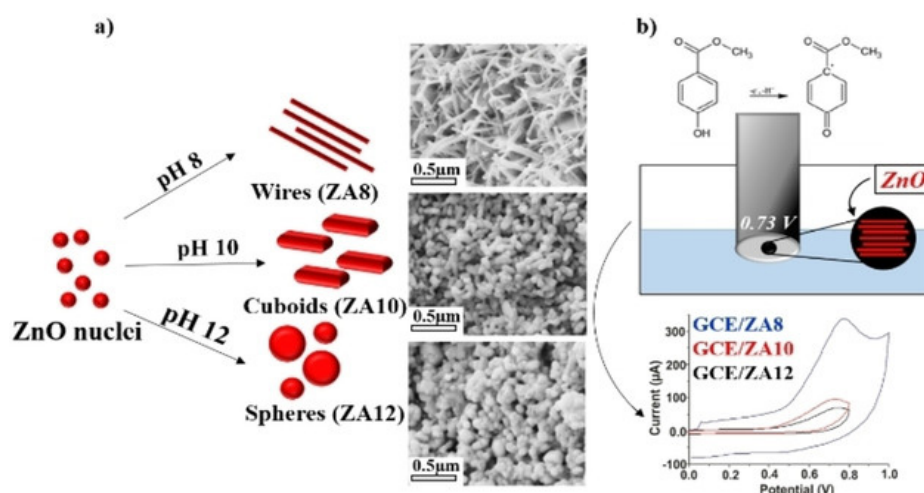


**Figure 5.** Schematic illustration of the proposed mechanism for (a) the growth of ZnO NPs at pH 8, 10, and 12 with their respective SEM images and (b) the electrochemical detection of MePa in an aqueous solution using three reported morphologies. Reproduced from reference [122] with permission from John Wiley and Sons, copyright 2021.

The use of screen-printed electrodes for developing sensors for estrogens has been reviewed recently [123] and progress in the development biosensors, including those based on optical and spectroscopic approaches, has also recently been reviewed [124]. Molecular imprinting combined with nanoparticle layers has been another avenue for development. Other strategies reported for electrode modification have included GCE modified with Pt nanoparticles and then by a molecularly imprinted polymer layer [125]. PtNP were first formed on the GCE by electrodeposition and then the layer of PtNP surface modified by the monomer 6-mercaptopnicotinic acid which also served as the monomer for electropolymerization. The electropolymerization took place in the presence of the 17 $\beta$ -estradiol, which was subsequently washed out, leaving behind a molecularly imprinted surface. Ten cycles of electropolymerization gave a layer with a thickness that gave the optimal response. A ratio of monomer:E2 of 24:1 was found to produce a surface of optimal response. An incubation time of 4 min was found to be optimal. A linear range in DPV response was found for oxidation of E2 just below 0.7 V (vs. SCE) over a range of 0.03–50.0  $\mu\text{M}$  with a detection limit of 0.016  $\mu\text{M}$ . GCE modified by electrodeposited Au nanoparticles and then

covered by a molecularly imprinted polymer layer was used to develop and electrode for estradiol detection [126]. In a similar strategy, 4-aminothiophenol was self-assembled onto the layer of AuNPs and then used as the monomer for electropolymerization in the presence of estradiol that was subsequently washed out. An incubation time of 8 min was found to be optimal with a range from 1–15 min tested for maximum current in chronoamperometric detection ( $-0.3$  V vs. Ag/AgCl, 200 s). The imprinted sensor was characterized using CV and EIS and the  $\text{Fe}(\text{CN})_6^{3-/4-}$ . The linear range was reported as  $1.0 \times 10^{-12}$  mg mL $^{-1}$  to  $1.0 \times 10^{-8}$  mg mL $^{-1}$  with a detection limit of  $1.28 \times 10^{-12}$  mg mL $^{-1}$ . Milk samples spiked with E2 showed recoveries from 84.7–102.9%.

Oral contraceptives also constitute a problem for environmental contamination and cause endocrine-disrupting effects. 17- $\alpha$ -ethynylestradiol (EE2) is used in contraceptives and hormone replacement and is a potentially significant environmental contaminant [127]. Magnetic nanoparticles of  $\text{Fe}_3\text{O}_4$  (10–15 nm) modified by molecularly imprinted siloxane polymer (mag@MIP) were used to capture EE2 from solution and then these particles were magnetically bound to an SPCE modified by graphene that had been treated with strong acid (functionalized graphene) and by graphene quantum dots to enhance electrical conductivity. The surface area of the magnetic nanoparticles was enhanced by about 50% due to the imprinting step. An analyte adsorption time onto dispersed mag@MIP of 3.0 min was found to be optimal. The amount of dispersed mag@MIP was also optimized. SWV showed an oxidation peak for EE2 near 0.26 V (vs. Ag/AgCl) and a limit of detection of 2.6 nM was found with a linear range from 10 nM to 2.5  $\mu\text{M}$ . Recovery of samples from EE2 spiked into urine, serum, and river water was found to be excellent.

### 7.3. Application to Detection of Pharmaceutical CECs

Antibiotics are essential to human health as antiseptic and anti-inflammatory medications. However, a growing number of issues have come to light as a result of prolonged antibiotic use. Clinically, drug overdose can result in a variety of negative side effects, including nausea, vomiting, abdominal pain, and lack of appetite. The quantity of antibiotics is especially crucial. The liver or kidneys are typically where many antibiotics are processed, which may cause organ damage [128]. Unneeded or outdated products from the pharmaceutical industry and clinics were presumably being immediately dumped to ecosystems and water bodies. Due to their poor solubility over time, the metabolites of micropollutants pose a serious health danger to both aquatic life and people [129].

The antibiotic tinidazole, which is 1-(2-ethyl sulfonyl ethyl)-2-methyl-5-nitro-imidazole, can be an environmental contaminant and be cytotoxic, carcinogenic, and mutagenic in humans. An electrochemical sensor for tinidazole was developed using an Ag- $\text{Co}_3\text{O}_4$  nanomaterial as an electrocatalyst to modify a GCE [130]. Under SEM, the prepared nanomaterial showed ‘carrom coin’ disc-like structures of  $\text{Co}_3\text{O}_4$  decorated by silver nanoparticles. EIS confirmed a much lower charge transfer resistance on the modified GCE. An irreversible reduction reaction was used to detect tinidazole using amperometry and the modified GCE as a rotating disc electrode in pH 7.0  $\text{N}_2$  saturated phosphate buffer. Two linear segments in the cathodic current density vs. concentration were observed with linearity up to 388  $\mu\text{M}$  and detection limit of 0.035  $\mu\text{M}$ . The sensor was selective against a range of likely interferent species and recovery was excellent for tinidazole spiked into a range of aqueous media, including drinking water, sewage water, lake water, and tap water.

The antibiotic metronidazole (MNZ) has been used in animal feed but in humans can cause seizures, ataxia, and peripheral neuropathy. An electrochemical sensor for metronidazole was assembled using molecular imprinting and the superior electrical conductivity properties of graphene quantum dots [131]. Graphene nanoplatelets were drop-cast onto GCE to improve surface conductivity. A nanocomposite of graphene quantum dots and molecularly imprinted siloxane polymer was then drop-cast. MNZ was removed by solvent wash until it was no longer detected by UV-visible spectrometry. In CVs, the peak current was  $2.1 \times$  higher for the modified electrode than for MNZ on bare GCE. MNZ was found to undergo a  $4\text{H}^+$ ,  $4\text{e}^-$  reduction reaction on the electrode. An accumulation time of 80 s was

found to be optimal with no further current increase at longer times. A detection limit of 0.52 nM was found with a linear range in two regions from 0.005–0.75 and 0.75–10.0  $\mu\text{M}$ .

Antibiotics released into the environment can put animals at risk of cancer. The antibiotics sulfamethoxazole and trimethoprim are frequently used together in a synergistic manner. A GCE modified with a 3:1 by weight mixture of ZnO nanorods (~ 180–250 nm diameter and 1.4  $\mu\text{m}$  in length) and graphene by drop-casting was found to perform well for simultaneous detection of these two antibiotics [132]. The ZnO nanorods possessed good electron transport properties and prevented the graphene sheets from aggregating by intercalation between the ZnO nanorods. EIS showed that the addition of graphene greatly reduced the charge transfer resistance relative to that of GCE modified only with ZnO nanorods. The detection using DPV showed two oxidation peaks for each compound, with one peak much larger than the other. Two linear ranges were observed, with the second extending to 220  $\mu\text{M}$  for sulfamethoxazole and to 180  $\mu\text{M}$  for trimethoprim. Detection limits of 0.4  $\mu\text{M}$  for sulfamethoxazole and 0.3  $\mu\text{M}$  for trimethoprim were reported. Excellent recovery was found when samples were spiked into aqueous media, including lake water. While lower limits of detection for these two antibiotics have been reported, this approach produced a wider linear range.

Sulfamethoxazole and trimethoprim are both antibiotics of concern as environmental contaminants and their residues can cause thyroid cancer. A sensor for sulfamethoxazole (SMX) and trimethoprim (TMP) was developed by first preparing  $\text{Fe}_3\text{O}_4$  nanoparticles in the presence of a dispersion of MWCNT by precipitation by reaction of  $\text{FeCl}_3$  and  $\text{Fe}_3\text{O}_4$  with  $\text{NH}_4\text{OH}$ . The MWCNT and  $\text{Fe}_3\text{O}_4$  nanoparticles were then drop-cast onto GCE. EIS showed that GCE/MWCNT/ $\text{Fe}_3\text{O}_4$  nanoparticles electrode had the best electron transfer properties with low charge transfer resistance and low phase angle in a Bode plot. CV on GCE showed well-separated irreversible anodic peaks for SMX (914 mV, vs. Ag/AgCl) and TMP (1150 mV, vs. Ag/AgCl) that were amplified by a factor of 3.5 upon modification with MWCNT/ $\text{Fe}_3\text{O}_4$  and were at a lower potential by a few hundred mV than seen on bare GCE. DPV was used for simultaneous determination of SMX and TMP and measured up to 0.5  $\mu\text{M}$ . The detection limit for SMX was found to be 11.0 nM and that for TMP was 21.0 nM [133].

The detection of acetaminophen and estrogen in water was achieved using GCE modified by multi-walled carbon nanotubes (MWCNT) modified with  $\beta$ -cyclodextrin in four different ways: physical mixing, use of a click chemistry reaction, esterification using thionyl chloride, and a one-step Steglich esterification. 4-ethynylaniline was used to modify MWCNTs to present alkyne groups. The goal was to take advantage of the complexation ability of  $\beta$ -cyclodextrin and the excellent conductivity of MWCNTs. The MWCNT dispersions were drop-cast on GCE, followed by heating at 80  $^\circ\text{C}$ . Linear sweep voltammetry was applied to detection of acetaminophen over the range 0.005–20  $\mu\text{M}$  and of estrogen (17 $\beta$ -estradiol) over the range 0.01–15  $\mu\text{M}$ . The greatest slope for peak current versus concentration was found for the electrode prepared using MWCNT linked to  $\beta$ -cyclodextrin using the one-step Steglich esterification that makes use of the reagents dicyclohexylcarbodiimide (DCC) and 4-dimethylaminopyridine (DMAP). The slope was 1.8  $\mu\text{A } \mu\text{M}^{-1}$  for these electrodes versus 1.27  $\mu\text{A } \mu\text{M}^{-1}$  for the electrode modified by MWCNT and  $\beta$ -cyclodextrin physically mixed. Detection limits of 3.3 and 2.5 nM were found for acetaminophen and 17 $\beta$ -estradiol, respectively [134].

Non-steroidal anti-inflammatory drugs (NSAIDs) such as naproxen when released into aquatic ecosystems pose a serious threat to aquatic animals. GCE modified by a ternary nanocomposite of Au nanoparticles with carbon nanotubes surface-modified to present carboxylic acid groups and graphene oxide [135]. SEM indicated Au nanoparticles situated around the edges of the –COOH functionalized carbon nanotubes and next to graphene oxide sheets. A scheme showing the synthesis of this nanocomposite is shown below in Figure 6. EIS showed that the full ternary nanocomposite modified electrode showed the lowest charge transfer resistance. Chronoamperometry was applied to naproxen in 0.1 M PBS over the range of concentration of 0.1–113.6  $\mu\text{M}$  at 1.1 V (vs. Ag/AgCl) and a limit of detection of 14 nM was found. The selectivity was found to be good in the

presence of excess concentrations of potential interferents such as fructose, sucrose, glucose, acetaminophen, chloramphenicol, nitrite, and NaCl. Recovery from samples spiked into media including tap water, sea water, river water, and pond water was near 100%.

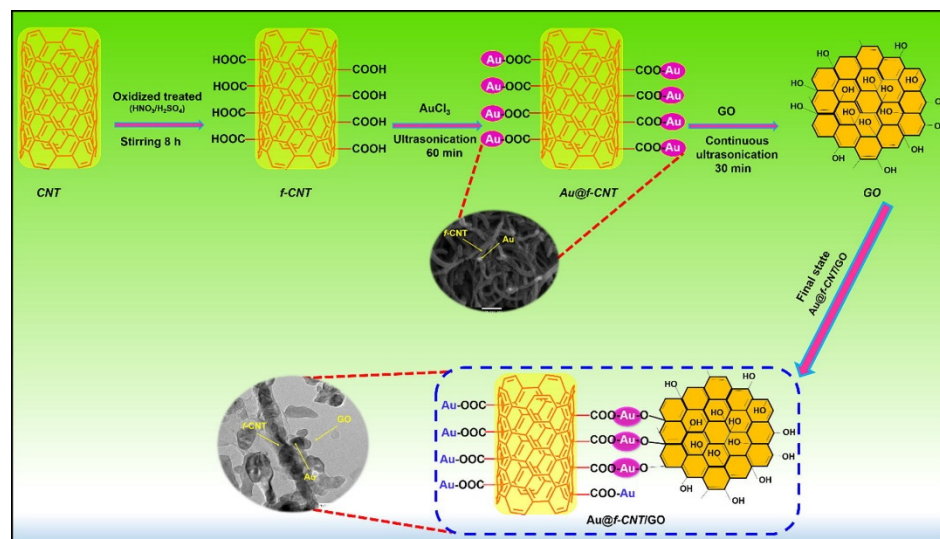


**Figure 6.** Overall synthesis of Au@f-CNT/GO hybrid nanocomposite via ultrasonication. Reproduced from reference [135] with permission from Elsevier, copyright 2021.

The detection of the antibiotic ciprofloxacin and the anti-pyretic and analgesic paracetamol was reported using a graphite electrode modified with  $\text{TiO}_2$  sol also containing CMK-3 mesoporous silica, gold nanoparticles and Nafion. Mesoporous silica was used to enhance the surface area and gold nanoparticles and Nafion contributed excellent conductivity [136]. Using currents in CV measured at 400 mV and at 700 mV (vs. Ag/AgCl) in solution, two linear ranges of 1–10  $\mu\text{M}$  and then 10–52  $\mu\text{M}$  were reported for each compound. Detection limits of the 0.108 and 0.210  $\mu\text{M}$  were determined for ciprofloxacin and paracetamol, respectively. Recovery was excellent for samples spiked into river water or wastewater.

Screen-printed carbon electrodes modified by carbon nanofibers were used to develop a sensor for paracetamol based on analyte adsorption followed by stripping voltammetry for detection [137]. Linear ranges from 2.0–50 nM and from 0.1–2.0  $\mu\text{M}$  were observed, and a very low detection limit of 0.54 nM was reported. Theoretical modeling found that the paracetamol adsorbed parallel to the carbon surface with a binding energy of  $-68$  kJ/mol. Selectivity against common interferents, including a range of metal ions, ibuprofen, and caffeine, was very good, and recovery from samples spiked into sea and river water was near 100%.

Antidepressants such as citalopram are also known as dangerous contaminants of aquatic environments. A nanocomposite of metal–organic framework (JUK-2 MOF), together with MWCNTs and Au nanoparticles, was used to modify GCE to create a sensor for citalopram [138]. JUK-2 is a proton-conducting MOF. The lowest charge transfer resistance was found for GCE modified with the complete nanocomposite layer. Staircase voltammetry was found to be the most suitable method of detection, and the anodic peak current for irreversible oxidation was found to display three distinct and successive linear ranges of 0.05–1.0  $\mu\text{M}$ , 1.0–10  $\mu\text{M}$ , and 15.0–115  $\mu\text{M}$ , with sensitivities of 38.0, 15.89, and 3.32  $\mu\text{A } \mu\text{M}^{-1}$ , respectively. The reported detection limit was 0.011  $\mu\text{M}$ . The recovery for samples spiked in river, surface, and wastewater was excellent.

Chlorpromazine is an antipsychotic drug which, upon continued exposure, can lead to many disorders such as tardive dyskinesia, vision changes, neuromuscular problems, and contact dermatitis. An electrochemical sensor for this drug was developed, taking advantage of the cubic  $\beta$ -phase of stannous tungstate since it has high catalytic activity

and was used in the form of one-dimensional nanorods prepared using a sonochemical method. TEM showed the nanorods to be 40 nm wide and 300–350 nm long, and the material was further characterized by EDS mapping, FTIR, XPS, and powder XRD. The  $\beta$ -SnWO<sub>4</sub> nanorods were drop-coated over the GCE [139]. The amperometric current versus concentration was increased by successive additions of chlorpromazine in pH 7.0 phosphate buffer, measured using the modified GCE as a rotating disc electrode at 1200 rpm and 0.65 V (vs. Ag/AgCl). This current was found to increase linearly from 0.01 to 457  $\mu$ M chlorpromazine with a detection limit of 0.003  $\mu$ M. Selectivity against a range of common interferents was excellent, and so was reproducibility among five different prepared electrodes and ten trial runs using the same electrode.

Cobalt oxide, Co<sub>3</sub>O<sub>4</sub>, is a p-type semiconductor with high electrochemical activity. Nanocubes of Co<sub>3</sub>O<sub>4</sub> doped with La<sup>3+</sup> were prepared by autoclaving a solution of the precursor salts together with polyvinylpyrrolidone (PVP). The nanocubes were about 70 nm in size and were drop-cast over a screen-printed electrode and used to make a sensor for the antidepressant drug venlafaxine. Cyclic voltammograms of venlafaxine in pH 7.0 PBS showed an irreversible oxidation near 0.70 V (vs. Ag/AgCl). The peak current increased linearly with the square root of the scan rate as expected for diffusion-controlled behavior. Using DPV, a linear range from 1.0–500  $\mu$ M was found with a detection limit of 0.5  $\mu$ M. Recovery of samples spiked into drinking water, wastewater, and river water was near 100%. Interference of less than 5% was reported for a wide range of potential interfering species including, based on obtained results, Mg<sup>2+</sup>, Al<sup>3+</sup>, NH<sub>4</sub><sup>+</sup>, F<sup>-</sup>, SO<sub>4</sub><sup>2-</sup>, S<sup>2-</sup>, caffeine, urea, ethanol, methanol, benzoic acid, fructose, saccharose, tyrosine, lactose, L-phenylalanine, L-tryptophan, L-glycine, L-histidine, L-proline, L-threonine, L-serine, L-asparagine, uric acid, acetaminophen, NADH, dopamine, ascorbic acid, epinephrine, norepinephrine, glucose, and L-lysine [140].

#### 7.4. Application to Detection of CECs of Agricultural Use

Horticulturists and farmers commonly employ insecticides to keep unwanted critters at bay. Pesticides have many practical applications in agriculture, but they are not without their downsides. The massive use of pesticides and the lack of expertise in their application have contaminated land and water. Dosage limits and monitoring at the trace level are essential for lessening pesticides' negative effects. The development of new, sensitive, selective, and straightforward methods for determining the lowest feasible concentrations of pesticides is thus critically important [141]. Detection of the pesticide carbofuran was achieved using DPV and a GCE modified with a composite of reduced graphene oxide (rGO) and Au nanoparticles subsequently covered by a layer of a molecularly imprinted polymer. The rGO/Au nanoparticles were dispersed in Nafion before a small volume was drop-cast onto GCE. Methyl acrylic acid, ethylene glycol maleicrosinate acrylate as cross-linker, and AIBN as free radical initiator in toluene along with carbofuran were drop-cast over the composite and allowed to react at 353 K in a vacuum oven for 4 h, followed by washing out the carbofuran template. Upon incubation with carbofuran, the current due to the Fe(CN)<sub>6</sub><sup>3-/4-</sup> redox couple was reduced as the pesticide molecule bound into the imprinted sites and hindered electron transfer of the redox probe. The calibration curve was found to decrease from 50 nM to 20  $\mu$ M, and a detection limit of 20 nM was reported. The sensor was selective against structurally-related analogs of carbofuran [142].

A sensor for organophosphorous pesticides was achieved by forming CuO nanoflowers on ITO electrodes using a hydrothermal synthesis. The distinct microns-wide flower-like morphology was composed of units of nano-beads in the 20–70 nm size range. Pimelic acid was added to act as an agent to direct the orientation of the CuO nuclei. SEM observation showed full coverage of the ITO surface by CuO nanoflowers of about 34  $\mu$ m thickness. Pralidoxime chloride was immobilized over the pimelic acid on the CuO nanoflowers. The oxidation of the aldoxime group of pralidoxime to carbonyl near 0.6 V (vs. Ag/AgCl) was inhibited by interaction with the pesticide molecules. Using the decrease in the oxidation current in DPV as the sensor response, calibration plots were determined for chlorpyrifos,

methyl parathion, and fenthion over the range 0.01–0.16  $\mu\text{M}$ . Detection limits of 1.6, 6.7, and 2.5 nM were found for chlorpyrifos, methyl parathion, and fenthion, respectively, which was lower than others reported, except for one for fenthion using pralidoxime on graphene quantum dots-modified electrodes [143].

Sensitive detection of the pesticide malathion was achieved using GCE modified with Pd@Au core-shell nanowires then covered by the enzyme acetylcholinesterase in a chitosan film. The Pd@Au nanowires were 7 nm wide and about a micron in length and formed a network-like pattern when drop-cast on GCE. DPV was used to detect the decrease in peak current for oxidation of thiocholine produced by the action of the enzyme on acetylthiocholine substrate upon inhibition by increasing amounts of malathion. A linear range of 0.1 pM–100 nM was found with a detection limit of 0.037 pM. Recovery of malathion spiked in tap water was near 100% [144].

Acetaprimid is a broad-spectrum insecticide and is of concern as an environmental contaminant. Although acetaprimid is electrochemically inactive, a sensor could be developed using EIS. Au nanoparticles of 50 nm diameter were formed by electrodeposition onto an Au electrode surface. The aptamer specific for acetaprimid was thiol-terminated, and the formation of the Au nanoparticles on the Au electrode increased the surface loading of the aptamer ten-fold over that on the plain Au electrode [145]. 6-mercaptohexanol was used as a filler in-between immobilized aptamers. The charge transfer resistance ( $R_{ct}$ ) using redox probe  $\text{Fe}(\text{CN})_6^{3-/4-}$  increased linearly with  $\log C$  over the range 5–600 nM. The detection limit was found to be 1 nM. The sensor was highly selective in the presence of a variety of pesticides, and recovery for samples spiked into wastewater was close to 100%.

A sensor for the herbicide aminotriazole was developed based on  $\text{TiO}_2$  nanoparticles and surfactant cetyltrimethylammonium bromide (CTAB) added onto a carbon paste electrode (CPE) prepared from carbon powder and paraffin oil. The  $\text{TiO}_2$  particles were just below 100 nm in size. An irreversible anodic wave due to oxidation of aminotriazole (3-amino-1,2,4-triazole) to 3-amino-1,2,4-triazolone was seen near 0.91 V (vs. Ag/AgCl) and was about five-fold enhanced for the modified CPE than for unmodified CPE. A detection limit of 2.53 nM was reported, lower than almost all other electrochemical detection schemes previously reported for aminotriazole. The recovery of aminotriazole spiked into dam, pond, lake, and tap water, and RO (reverse osmosis) water was excellent [146].

Pralidoxime serves as an antidote for pesticide inhibition of acetylcholinesterase and is electrochemically active. The binding of non-electroactive organophosphorus pesticides (OPP) to pralidoxime prevents the irreversible oxidation of the aldoxime group, and this can be used as the basis for an electrochemical sensor [147]. The pralidoxime is a nucleophile and a nucleophilic substitution reaction with OPP occurs. An electrochemical sensor for non-electroactive OPP was constructed by drop-casting graphene quantum dots (average size 4.2 nm) in solution with chitosan onto GCE, followed by adsorption of pralidoxime which strongly was adsorbed by  $\pi$ - $\pi$  stacking and electrostatic interactions. The addition of OPP such as fenthion progressively suppresses the current peak for the oxidation of the aldoxime. Using the approach for the detection of fenthion with DPV gave a linear dependence of change in current ( $\mu\text{I}$ ) with  $\log C$  from  $10^{-11}$  to  $5 \times 10^{-7}$  M and a detection limit of 6.8 pM. Dichlone is a broad-spectrum fungicide and is also used as an algicide that is of environmental concern. The doping of ZnO nanoparticles with  $\text{Ca}^{2+}$  increases the conductivity and enhances the number of adsorption sites.  $\text{Ca}^{2+}$ -doped ZnO nanoparticles of near 200 nm diameter were prepared by co-precipitation followed by calcining and then mixed with carbon powder and paraffin oil to create a carbon paste electrode (CPE) [148]. Dichlone was added to soil samples that were then immersed in water and were added to natural water samples. In CV experiments, dichlone showed reversible redox behavior associated with  $2e, 2\text{H}^+$  reaction between the quinone and dihydroxy forms. Detection on CPE using SWV resulted in a detection limit of 59.8 nM and a linear range up to near 0.3  $\mu\text{M}$ . The SWV sweeps and the calibration plot for this sensor is shown in Figure 7. Recovery from natural water samples and soil samples was near 100%. The CPE sensor retained 90–94.6% of its original signal after 10 days of storage.

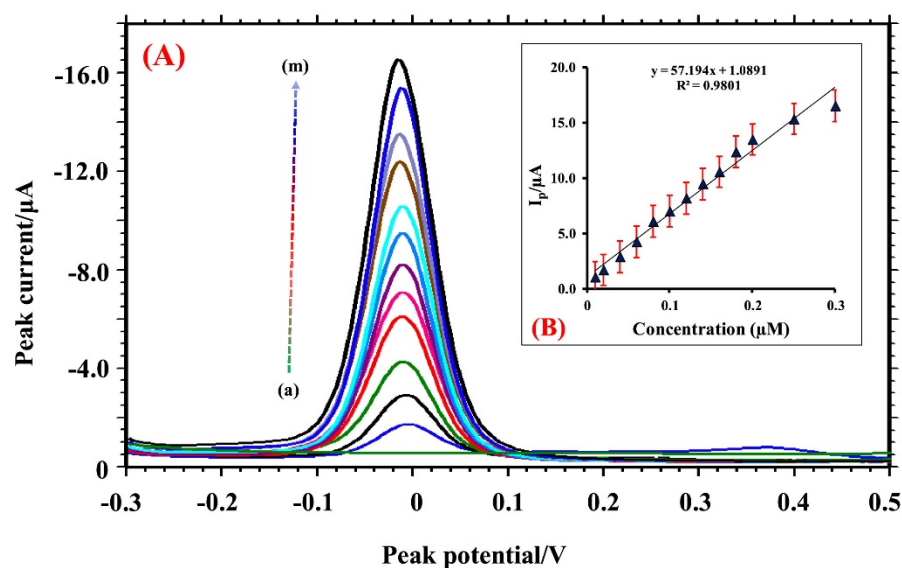


**Figure 7.** (A) SWV response at various concentration level of DCN (a) blank, (b) 10 µM, (c) 20 µM, (d) 40 µM, (e) 60 µM, (f) 80 µM, (g) 100 µM, (h) 140 µM, (i) 180 µM, (j) 220 µM, (k) 260 µM, (l) 300 µM, (m) 350 µM. Inset (B) calibration plot. Reproduced from reference [148] with permission from Elsevier, copyright 2022.

Nanoporous gold prepared by dealloying of 12 karat Au leaf (50% Au) was fixed on the surface of a GCE and used to create a sensor for fungicide carbendazim (CBM) and pesticide methyl parathion (MP) [149]. The NPG layer was about 100 nm thick with pores of 35 nm size. DPV in pH 4.0 acetate buffer that was deoxygenated showed oxidation peaks at 0.25 V for MP and 0.95 V for CBM (vs. SCE). The linear range used was 0.5–150 µM for MP and 3–120 µM for CBM. Detection limits of 0.02 µM were found for MP and of 0.24 µM for CBM. The sensor was applied to samples spiked into wastewater and seawater and selectivity in the presence of five other pesticides was excellent, as was sample recovery.

### 7.5. Applications to Other CECs

It is imperative that efficient, fast, and reliable analytical techniques with adequate detectability to quantify a variety of synthetic pigments and dyes, which are becoming increasingly dispersed throughout the environment, be developed. This is because they have a substantial impact on the environment and can cause toxic effects. Electrochemical detection of reactive Red 195 from industrial waste samples was performed on a graphene-modified GCE utilizing bare and surface-altered GCE at pH values ranging from 1.0 to 13.0 with 4.0 found to be the optimal pH. At pH 4.0, RR 195 showed strong linear responses on both electrodes. Calibration plots were also created varying concentration of the dye, and other parameters including accumulation potential, accumulation time, initial scan potential, pulse height, pulse breadth, and potential scan increment and scan rate were optimized. The stripping voltammetric activity of the dye on a graphene-coated electrode had an extremely low detection threshold of 30 ppb. Atomic force microscopy verified the compound's adsorption on GCE and graphene-coated GCE [150].

Fire suppression foams, nonstick cookware, water-resistant clothes, and personal care items can all include per- and polyfluoroalkyl substances (PFAS), a new and persistent class of environmental micropollutant. Due to the durability of their network of carbon-fluorine linkages, PFAS have very slow biodegradation kinetics. Mammals exposed to PFAS have been proven to experience a wide range of harmful health effects, including hypertension, thyroid disturbance, immunotoxicity, reproductive toxicity, and hepatotoxicity. Additionally, it has been discovered that PFOS, PFOA, and other PFAS exhibit many of the essential traits of carcinogens, including changing oxidative stress, immunosuppression, and modification of receptor-mediated effects [151]. Approaches to detection of PFAS using

electrochemical methods have so far focused on molecularly imprinted polymer layers and not yet on nanomaterials.

Sodium dodecyl sulfate (SDS) is an anionic surfactant that may be toxic to aquatic organisms, especially during fish fertilization, and also affects the health of the kidneys and spleen. To detect SDS, Faradilla et al. developed electrochemical sensing based on screen-printed carbon electrode (SPCE) modified with ZnO NPs/MIP. The ZnO NPs/MIP were manufactured on the SPCE substrate using a straightforward and efficient drop-casting process. On the developed electrode, the linear dynamic range for detection of SDS was 1–10  $\mu\text{M}$ , and the limit of detection was 0.652  $\mu\text{M}$ . Similar responses after 10 iterations of DPV testing confirm the designed electrode's repeatability performance. Perhaps most intriguingly, coupling the MIP with ZnO NPs increases the current response of SDS by a factor of up to four. The suggested SPCE-ZnO NPs/MIP shows promise for direct environmental monitoring of SDS due to its high percentage recovery of SDS from real samples [152].

Bansal et al. conducted research on electrochemical sensors based on  $\text{ZrO}_2$  NPs/Au electrode sensing layer for monitoring hydrazine and catechol in real water samples [153]. Toxicity and limited degradability make them environmental dangers. Hydrazine is an EPA-listed neurotoxic and carcinogen. Pharmaceuticals, photography, fuel cells, insecticides, corrosion protection, and rocket propellant use it. CT is used to make insecticides, fragrances, and drugs. The purpose of the current study is to investigate the electroanalytical uses of  $\text{ZrO}_2$  NPs for the detection of hazardous compounds in industrial effluent stream and other sources. Using a highly effective  $\text{ZrO}_2$ /Au hybrid electrode, catechol and hydrazine were electrochemically detected using chronoamperometry. The fabricated system's limit of detection, sensitivity, and reaction time were all found to be excellent. With respect to hydrazine and catechol, the sensor showed good sensitivity, measuring 8.99 and 0.14  $\mu\text{A } \mu\text{M}^{-1} \text{ cm}^{-2}$ , respectively. It was discovered that the  $\text{ZrO}_2$  NPs catalyzed the oxidation and reduction of catechol. It was found that the sensor was selective for hydrazine and catechol. The sensing platform was also shown to be an effective method for detecting catechol and hydrazine in samples spiked into water. The limits of detection for hydrazine and catechol were found to be 1.05 and 7.68  $\mu\text{M}$ , respectively.

Shetti and coworkers developed a modified electrode for the detection of triclosan (5-chloro-2-(2,4-dichlorophenoxy)phenol), which is used in personal care products, including lotions, soaps, and shampoos, amongst many others, and serves as a antimicrobial, antifungal, and antibacterial agent [154]. Triclosan is stable and lipophilic and toxic to aquatic life and can also cause adverse reactions in humans. A carbon paste electrode was developed using  $\text{WO}_3$  nanorod structures (100–700 nm long and 50–100 nm wide) combined with reduced graphene oxide nanoparticles. The electrocatalytic properties of  $\text{WO}_3$  that arise from the presence of oxygen vacancies were combined with the excellent conductivity of rGO nanoparticles. The  $\text{WO}_3$  nanomaterials were characterized using XPS, SEM, and STEM (scanning transmission electron microscopy). Figure 8 shows the electron micrographs and the XRD spectrum for the  $\text{WO}_3$  nanostructures. The  $\text{WO}_3$ /rGO/CPE had a superior CV current response to triclosan in pH 9.2 phosphate buffer compared to rGO/CPE and  $\text{WO}_3$ /CPE. The oxidation of triclosan was found to depend on pH since it is a  $1\text{e}^-$ ,  $1\text{H}^+$  process. Using DPV, with oxidation of triclosan occurring near 0.6 V (vs. Ag/AgCl), gave a detection limit of 0.24 nM and a linear range from 10 nM–1.6  $\mu\text{M}$ . The recovery was excellent for triclosan spiked into soil samples, water (including dam water), and vegetable and fruit samples. Figure 8 is an image depicting the SEM images of  $\text{WO}_3$  in low and high resolutions and XRD pattern of  $\text{WO}_3$ .

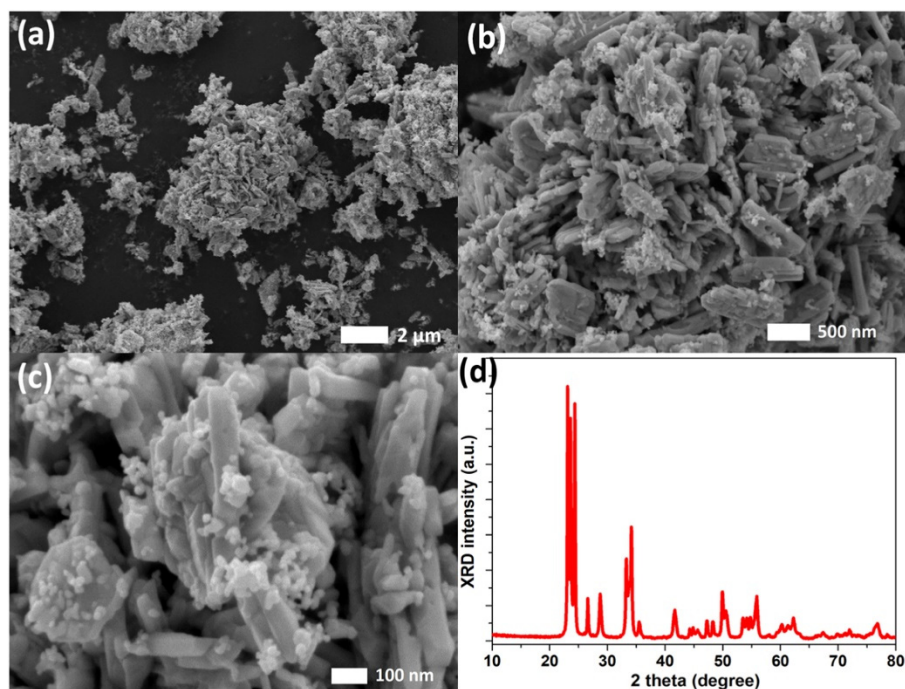


**Figure 8.** SEM images of  $\text{WO}_3$  in low (a) and high (b,c) resolutions. (d) XRD pattern of 1-D  $\text{WO}_3$  revealing monoclinic phase. Reproduced from reference [154] with permission from Elsevier, copyright 2022.

Brominated flame retardants have been the targeted analyte for a few studies to develop nanostructure modified electrodes. These compounds are used to reduce risk of fire but, when released into the environment, can have endocrine-disrupting properties, immunotoxicity, and neurotoxicity. A sensor for monobrominated 3-bromobiphenyl (3-BB) was constructed using an antibody specifically produced in inoculated rabbits [155]. An ITO electrode was modified with Au nanoclusters and then modified with polydopamine, followed by conjugation to the antigen by Michael addition reaction. A competitive electrochemical immunoassay was then performed by incubation with antigen and carbon hollow nanochains modified with horseradish peroxidase and anti-3-BB antibody. A linear response of the current due to HRP activity to 1 mM hydroquinone versus  $\log [3\text{-BB}]$  was found over the range 1 pM to 2 nM with a detection limit of 0.5 pM. The nanostructured surface and the increased enzyme loading on a nanocarrier each served to increase the response. A sensor for polybrominated tetrabromobisphenol A (TBBPA) was developed using a carbon electrode first modified with aniline and then covered by graphene oxide reduced to graphene and then covered by electrodeposited nickel nanoparticles [156]. Molecular imprinting was carried out using pyrrole and TBBPA. The sensor used DPV and  $\text{Fe}(\text{CN})_6^{3-/4-}$  as a probe, achieving a reduction in current with TBBPA concentration that was linear in  $\log[\text{TBBPA}]$  over the range from 0.5 nM–10  $\mu\text{M}$ , and with a detection limit of 0.13 nM. Recovery from samples in tap, rain, and lakewater was excellent.

The detection of monohydroxylated polyaromatic hydrocarbons was achieved using a screen-printed carbon electrode onto which graphene oxide had been reduced resulting in a porous nanostructure [157]. The three analytes were 2-hydroxynaphthalene, 3-hydroxyphenanthrene, and 1-hydroxypyrene, and all found to be electroactive and with distinct potentials such that all three could be distinguished when mixed. The compounds underwent  $\pi$ - $\pi$  stacking interactions on the electrode surface and the effect of accumulation time up to 60 min was investigated finding saturation after 40 min. Using DPV, linear ranges for 50–800 nM, 50–1150 nM, and 100–1000 nM were found for 2-hydroxynaphthalene, 3-hydroxyphenanthrene, and 1-hydroxypyrene, respectively. Detection limits of 10.1 nM, 15.3 nM, and 20.4 nM were found, respectively.

**Table 2.** Summary of different electrode modifications of electrodes, electrodes used, and electro-chemical sensing technique used in the detection of emerging contaminants.

| CEC                                  | Method of Detection | Surface Modification/Electrode                                     | LOD (nM)  | Linear Range ( $\mu\text{M}$ )    | Ref.  |
|--------------------------------------|---------------------|--|---|-----------------------------------|-------|
| <b>Bisphenol A (BPA) and related</b> |                     |  |   |                                   |       |
| BPA                                  | DPV                 | MCM-41 mesoporous silica + graphite + paraffin oil paste electrode | 38  | 0.22–8.8                          | [99]  |
| BPA                                  | DPV                 | MWCNT-COOH/Au NP on GCE  | 4.3   | 0.01–0.70                         | [100] |
| BPA                                  | DPV                 | Boron-doped diamond on GCE   | 5   | 0.1–50                            | [101] |
| BPA                                  | DPV                 | Carbon nanodiamond on GCE  | 0.5   | 0–30                              | [101] |
| BPA                                  | LSV                 | AuNPs/SGNF on GCE  | 0.0035  | 0.08–250                          | [102] |
| BPA                                  | DPV                 | Mo <sub>2</sub> Ti <sub>2</sub> AlC <sub>3</sub> /MWCNT on GCE     | 2.7   | 0.01–8.50                         | [103] |
| BPA                                  | DPV                 | MWCNTs/CuFe <sub>2</sub> O <sub>4</sub> NP on GCE                  | 3.2   | 0.01–120                          | [104] |
| BPA                                  | SWV                 | SH- $\beta$ -CD/NPGL on Au electrode                               | 10  | 0.3–100 (ln C)                    | [105] |
| Bisphenol S                          | DPV                 | Graphene and C60 on GCE  | 500   | 1–100                             | [106] |
| BPA                                  | EIS                 | Graphene + recombinant protein–BPA binding peptide on GCE          | $5 \times 10^{-6}$                              | $10^{-7}$ – $10^{-2}$             | [107] |
| BPA                                  | DPV                 | Chitosan + CNT + TiO <sub>2</sub> NP paste electrode               | 9.58  | 0.01–6.0                          | [108] |
| BPA                                  | EIS                 | Chitosan + CNT + TiO <sub>2</sub> NP paste electrode               | 7.012   | 0.01–6.0                          | [108] |
| BPA                                  | DPV                 | HS-ssDNA-wrapped SWCNT on Au                                       | 11.0  | 0.5–3.8                           | [109] |
| BPA                                  | DPV                 | SWCNT dispersed on Au  | 45.8  | 1–3.8                             | [109] |
| BPA                                  | DPV                 | MWCNT (d = 20–40 nm) on  | 84  | 4.9–82.5                          | [110] |
| BPA                                  | DPV                 | MWCNT (d = 110–170 nm) on  | 610   | 2.5–29.1                          | [110] |
| Bisphenol F and Bisphenol AF         | DPV                 | MWCNT–COOH on GCE  | $0.12 \times 10^6$<br>and<br>$0.17 \times 10^6$ | 600–1600                          | [111] |
| BPA                                  | DPV                 | AuPd NP/PDDA/MWCNT on GCE  | 60  | 0.18–18.0                         | [112] |
| <b>Estrogens</b>                     |                     |  |   |                                   |       |
| Hex                                  | DPV                 | HEX-AET-Au NPs on GCE  | 0.25 ng/mL                                      | 0.5–200                           | [116] |
| DE                                   | DPV                 | HEX-AET-Au NPs on GCE  | 0.25 ng/mL                                      | 0.50–2000                         | [116] |
| DNE                                  | DPV                 | HEX-AET-Au NPs on GCE  | 0.15 ng/mL                                      | 0.40–500                          | [116] |
| BPA                                  | DPV                 | HEX-AET-Au NPs on GCE  | 0.20 ng/mL                                      | 0.098–0.38                        | [116] |
| Estriol                              | DPV                 | Carbon nanoballs decorated with Ag NPs on GCE                      | 160   | 0.2–3.0                           | [117] |
| Diethylstilbesterol                  | DPV                 | Fe <sub>3</sub> O <sub>4</sub> -doped nanoporous carbon on GCE     | 4.6   | 0.01–12                           | [118] |
| 17- $\beta$ -estradiol               | DPV                 | Fe <sub>3</sub> O <sub>4</sub> -doped nanoporous carbon on GCE     | 4.9   | 0.01–20                           | [118] |
| 17- $\beta$ -estradiol               | DPV                 | Graphene nanoribbon + Au NP on fumed silica on GCE                 | 7.4   | 0.1–5.0                           | [119] |
| 17- $\beta$ -estradiol               | DPV                 | MWCNT-COOH on GCE  | 70  | 1.0–20                            | [120] |
| 17- $\beta$ -estradiol               | EIS                 | Zn NP/nanodendritic Au on Boron-doped diamond thin film electrode  | $5.0 \times 10^{-6}$                            | $10^{-8}$ to $10^{-3}$<br>(log C) | [121] |
| methylparaben                        | SWV                 | ZnO nanospheres + carbon black/Nafion on GCE                       | 8.99  | 20–80                             | [122] |
| methylparaben                        | SWV                 | ZnO nanocuboids + carbon black/Nafion on GCE                       | 7.76  | 30–80                             | [122] |
| methylparaben                        | SWV                 | ZnO nanowire + carbon black  | 7.25  | 20–120                            | [122] |
| 17- $\beta$ -estradiol               | DPV                 | MIP/Pt NP on GCE   | 16  | 0.03–50                           | [125] |

Table 2. Cont.

| CEC                    | Method of Detection | Surface Modification/Electrode   | LOD (nM)               | Linear Range ( $\mu\text{M}$ )              | Ref.  |
|------------------------|---------------------|--|------------------------|---|-------|
| 17- $\beta$ -estradiol | DPV                 | MIP/Au NP on GCE   | $4.7 \times 10^{-6}$   | $3.7 \times 10^{-9}$ – $3.7 \times 10^{-4}$ | [126] |
| Ethinlestradiol        | SWV                 | Fe <sub>3</sub> O <sub>4</sub> NPs@MIP on graphene quantum dot, graphene on SPCE | 2.6                    | 0.01–2.5                                    | [127] |
| 17- $\beta$ -estradiol | LSV                 | MWCNT- $\beta$ CD on GCE   | 2.5                    | 0.01–15                                     | [134] |
| <b>Pharmaceuticals</b> |                     |  |                        |   |       |
| tinidazole             | CA                  | Co <sub>3</sub> O <sub>4</sub> nano ‘carrom coin’/Ag NP on GCE RDE               | 35                     | 0–388                                       | [130] |
| metronidazole          | CV                  | MIP siloxane polymer on graphene quantum dots on graphene nanoplatelets/GCE      | 0.52                   | 0.005–0.75, 0.75–10.0                       | [131] |
| sulfamethoxazole       | DPV                 | ZnO nanorod + graphene on GCE  | 400                    | 0–220                                       | [132] |
| trimethoprim           | DPV                 | ZnO nanorod + graphene on GCE  | 300                    | 0–180                                       | [133] |
| sulfamethoxazole       | DPV                 | Fe <sub>3</sub> O <sub>4</sub> NP + MWCNT on GCE                                 | 21                     | 0–0.5                                       | [132] |
| trimethoprim           | DPV                 | Fe <sub>3</sub> O <sub>4</sub> NP + MWCNT on GCE                                 | 11                     | 0–0.5                                       | [133] |
| acetaminophen          | LSV                 | MWCNT- $\beta$ CD on GCE   | 3.3                    | 0.005–20                                    | [134] |
| Naproxen               | CA                  | Au NP/MWCNT-COOH/Graphene oxide on GCE   | 14                     | 0.1–113.6                                   | [135] |
| ciprofloxacin          | CV                  | TiO <sub>2</sub> sol/CMK-3 mesoporous silica/Au NP/Nafion on graphite electrode  | 108                    | 1–10, 10–52 (two ranges)                    | [136] |
| paracetamol            | CV                  | TiO <sub>2</sub> sol/CMK-3 mesoporous silica/Au NP/Nafion on graphite electrode  | 210                    | 1–10, 10–52 (two ranges)                    | [136] |
| paracetamol            | SV                  | Carbon nanofibers on SPCE  | 0.54                   | 0.1–2.0, 2.0–50 (two ranges)                | [137] |
| citalopram             | CV                  | MOF/Au NP/MWCNT on GCE   | 11                     | 0.05–1.0, 1.0–10 and 15.0–115 (3 ranges)    | [138] |
| chlorpromazine         | DPV                 | SnWO <sub>4</sub> nanorods on GCE on RDE   | 3                      | 0.01 to 457                                 | [139] |
| venlafaxine            | DPV                 | Co <sub>3</sub> O <sub>4</sub> nanoparticles/PVP on SPCE                         | 500                    | 1–500                                       | [140] |
| <b>Agrochemicals</b>   |                     |  |                        |   |       |
| carbofuran             | DPV                 | rGO/Au NP/MIP on GCE   | 20                     | 0.05–20                                     | [142] |
| chlorpyrifos           | DPV                 | CuO nanoflower on ITO  | 1.6                    | 0.01–0.16                                   | [143] |
| methyl parathion       | DPV                 | CuO nanoflower on ITO  | 6.7                    | 0.01–0.16                                   | [143] |
| fenthion               | DPV                 | CuO nanoflower on ITO  | 2.5                    | 0.01–0.16                                   | [143] |
| malathion              | DPV                 | Pd@Au core-shell nanowires in chitosan/GCE                                       | $0.037 \times 10^{-6}$ | $10^{-6}$ – $10^{-4}$                       | [144] |
| acetaprimid            | EIS                 | Au NP on Au  | 1                      | 0.005–0.6                                   | [145] |
| aminotriazole          | CV                  | TiO <sub>2</sub> NP + CTAB in CPE  | 2.53                   |   | [146] |
| fenthion               | DPV                 | Pralidoxime/graphene QD on GCE   | 0.0068                 | $10^{-5}$ –0.5 (log C)                      | [147] |
| Dichlone               | SWV                 | Ca <sup>2+</sup> -doped ZnO NP in carbon paste electrode                         | 59.8                   | 0–0.3                                       | [148] |
| carbendazim            | DPV                 | NPGL on GCE  | 240                    | 3–120                                       | [149] |
| methyl parathion       | DPV                 | NPGL on GCE  | 20                     | 0.5–150                                     | [149] |

Table 2. Cont.

| CEC                    | Method of Detection | Surface Modification/Electrode                           | LOD (nM) | Linear Range ( $\mu\text{M}$ )      | Ref.  |
|------------------------|---------------------|--|----------|-------------------------------------|-------|
| <b>Other CECs</b>      |                     |  |          |                                     |       |
| Red 95                 | DPV                 | Graphene/GCE   | 30 ppb   |                                     | [150] |
| SDS                    | DPV                 | ZnO NPs/MIP on SPCE                                      | 652      | 1–10                                | [152] |
| hydrazine              | CA                  | ZrO <sub>2</sub> NP on Au electrode                      | 1050     | 20–90                               | [153] |
| catechol               | CA                  | ZrO <sub>2</sub> NP on Au electrode                      | 7680     | 10–90                               | [153] |
| triclosan              | DPV                 | WO <sub>3</sub> nanorods + rGO in carbon paste electrode | 10       | 0.01–1.6                            | [154] |
| 3-bromobiphenyl (3-BB) | CV                  | 3-BB Antibody on Au nanoclusters on ITO electrode        | 0.0005   | 1 pM–2 nM, current vs. log[3-BB]    | [155] |
| tetrabromobisphenol A  | DPV                 | MIP (pyrrole) on Ni NP on graphene on CE                 | 0.13     | 0.0005–10.0, current vs. log[TBBPA] | [156] |
| 2-hydroxynaphthalene   | DPV                 | Porous reduced graphene oxide/SPCE                       | 10.1     | 0.05–0.800                          | [157] |
| 3-hydroxyphenanthrene  | DPV                 | Porous reduced graphene oxide/SPCE                       | 15.3     | 0.050–1.15                          | [157] |
| 1-hydroxypyrene        | DPV                 | Porous reduced graphene oxide/SPCE                       | 20.4     | 0.1–1.0                             | [157] |

MWCNT = Multi-walled carbon nanotube; NGF = Nanocomposite graphene film; HEX-AET-Au NPs-GCE = hexestrol (HEX)-2-aminoethanethiol hydrochloride (AET)-gold nanoparticles (Au NPs)-glassy carbon electrode; CNT-GCE = carbon nanotube-modified glassy carbon electrode; GR-ZnO/GCE = graphene (GR) and ZnO nanorods;  $\beta$ -CDs/MWCNTs/GCE =  $\beta$ -cyclodextrins and multi-walled carbon nanotubes; AuNP-SPCE = gold nanoparticle-modified screen-printed carbon electrodes; DNE = dienestrol; DE = diethylstilbestrol; Hexestrol = HEX; CV = Cyclic voltammetry; SWV = Square wave voltammetry; DPV = Direct pulse voltammetry; LSV = Linear Sweep Voltammetry; EIS = Electrochemical Impedance Spectroscopy; CA = chronoamperometry; SV = stripping voltammetry, ScV = staircase voltammetry; RDE = rotating disc electrode.

## 8. Conclusions

Improvements to the effectiveness of the many electrochemical sensing methods currently in use for the detection of CECs in air, soil, and, most crucially, groundwater, are urgently needed. In the past, chromatographic methods (HPLC, GC-MS) were used to quantify and detect CECs, but these techniques are labor-intensive and costly. Electrochemical techniques are the most ideal detection techniques that could be employed for sensing of these pollutants, while immunological assays like enzyme-linked immunosorbent assay (ELISA) are also used, however, they are not intended to be employed elsewhere other than at laboratories or research facilities and are much more time-consuming to conduct [1]. In this review, we discussed at length the modification procedures used to increase the selectivity and sensitivity of bare electrodes for sensing. GCE is the most represented electrode uses, with other forms of carbon-based electrodes also popular such as carbon paste. Also well-represented are ITO electrodes and, to a lesser extent, those of bare gold; however, it should be noted that nanoporous gold electrodes have appealing properties of high surface area and ease of modification that makes their further development in the future likely. It could be of special appeal to combine nanoporous gold electrodes with layers of nanocomposite materials. The primary difficulties with using the bare electrode surfaces of conventional electrodes for direct trace level detection are caused by the slow electrochemical kinetics on the surface and the low surface area of unmodified electrodes. It is difficult to detect analytes that have slow electrochemical oxidation using a conventional electrode. The typical electrode is not well-suited for simultaneously sensing multiple analytes due to slow electrochemical reactions [19].

We discussed a wide range of electrode modifications using nanostructures that have been introduced in recent years. The nanostructures available for use in the pursuit of developing electrochemical sensors for CECs have included gold nanoparticles, other gold nanostructures such as nanoporous gold, metal oxide nanoparticles, including those that

have been doped, and a variety of carbon nanostructures including graphene and carbon nanotubes. The introduction of the nanostructures onto the surface greatly enhances the amount of surface area, especially with metal oxide-related materials contributing many electroactive sites. Using nanostructures that are themselves of enhanced surface area such as nanowires, nanoflowers, or nanoporous particles can dramatically increase the surface area further. Many of these nanostructured electrodes are prepared on GCE based on its high conductivity. The composites applied to the electrode surface have been shown to gain in response when carbon nanostructures are added in addition to a reactive component such as a metal oxide nanoparticle or nanostructure. The metal oxide serves to provide active sites for analyte oxidation, while the carbon nanostructure serves to enhance the conductivity, promoting facile electron transfer and a greater current response.

A number of challenges can arise in the construction of nanoparticle/nanostructure modified electrodes for use in CEC. Stable attachment of the nanostructures onto the electrode surface is required for long-term stable use and reuse. The synthesis of the nanostructures must be reproducible as response parameters will vary with fine details of morphology and nanoscale dimensions. An additional concern would be difficulty in dispersing the nanostructures, especially nanoparticles, across the electrode surface or within an applied nanocomposite, since aggregation will reduce the number of exposed surface sites for analyte detection.

Additional and new nanomaterials that can enhance electrical conductivity and current response remain to be further explored in the development of these sensors. MXene materials are gaining in popularity as alternatives to graphene [158]. MXene materials are two-dimensional and consist of a transition metal (M), X is a C or N, and there is a terminal functional group such as  $-OH$ . MXene has excellent surface conductivity and served as a substrate for the polymerization of norepinephrine and deposition of Cu nanoparticles. The incorporation of MXene materials into nanostructured electrodes for detection of CECs is a trend that is likely to grow in future studies. Emerging work on the use of MXenes in developing modified electrodes for the detection of bromate ions, heavy metal ions, and some dyes has been recently reviewed [16].

When the electrodes are modified in an optimal way, CECs can be detected with high sensitivity, high selectivity, and adequate linear ranges. The vast majority of the reported sensors cover two decades of response and many cover up to five decades of response. A small number of the reported sensors respond with more than one linear range, with a change in the slope indicating a distinct change in response. For all of the studies presented here, the recovery of analyte from samples spiked into a variety of matrices including a range of natural water samples are reported as quite close to 100%. The electrochemical technique for determining their concentration is made practical by the reported absence of signal interferences, at least in terms of the common interferents examined. Because of their increased surface area and excellent catalytic properties, nanomaterials are a promising candidate in electrode modification, which in turn significantly alters the detection protocols for a wide range of environmental pollutants [9].

The time for the measurement of the analyte sample itself to take place in the case of DPV scans is quite short and is simply the potential range divided by the scan rate. A typical reported scan rate for DPV in these studies is  $10 \text{ mV sec}^{-1}$ , and if the potential window scanned is 600 mV then the time for the scan is 1 min. Small variations in times as short as this should not constitute a practical concern for analysis, and this is an advantage of determination using voltammetric scans using either LSV, DPV, SWV, or CV measurements. In a smaller number of studies, an accumulation time was employed for the analyte to adsorb onto the electrode prior to the scan and thus increase the signal. The use of an accumulation time clearly applies to sensors that combine nanostructures with a molecularly-imprinted polymer layer. The times noted are about 1–4 min, with the exception of monohydroxylated polyaromatic hydrocarbons as the analyte, for which times up to 60 min were considered [156]. For detection using the EIS method, a longer analysis time will be required, as the EIS data needed to produce a Zisman plot requires acquisition

over a wide frequency range of typically 1 mHz–10 kHz using Faradaic methods with the most commonly used  $\text{Fe}(\text{CN})_6^{3-/4-}$  redox probe. The total measurement time for an EIS spectrum can be 10 min or longer if even lower frequencies are included.

There are a number of avenues that should be pursued in the future to improve the efficacy of electrochemical approaches involving nanostructures for CEC detection. First, the use of rationally designed 2D and 3D nanomaterials for maximization of surface area, increase in the number of accessible active sites, and optimization of the structure of the nanoparticles involved will all be important. Experiments comparing the analytical parameters obtained for detection of a CEC that compare particle size, shape, dopant level, and nature of dopant are all advisable. The preparation of nanostructures in combination with supramolecular binding agents such as cyclodextrins, or other macrocycles for binding hydrophobic analytes, or with binding agents such as peptides or small molecules that can be surface-adsorbed securely and presenting properly spaced groups for hydrogen-bonding or stacking interactions, is a promising area for future development. Surface modification with electron transfer mediators that can reduce overpotentials for detection of certain CECs is also an area for potential development. The development of high throughput multi-array platforms for detection of several CECs simultaneously could result in the development of a portable, handheld instrument capable of rapid detection in the field [5]. These new sensors must be able to function using samples that may contain more than one CEC. Optimized modification of electrodes with nanostructures combined with rapid electrochemical detection using methods such as DPV with its low background current can greatly aid in the early in situ detection of these CECs in our ecosystems. A sweep of potential methods, including DPV, LSV, and SWV, will afford the most rapid detection, while methods such as EIS will require somewhat longer acquisition times as values of impedance are recorded at multiple individual frequencies and data analysis fitting to an equivalent circuit model is requiring typically to determine a charge transfer resistance. CV can be a simple and convenient method, although application of DPV or SWV is generally more sensitive and less subject to background currents. The detection of CECs before they accumulate and become environmental and health threats is vital, and further legislation concerning the use of these substances by regulating bodies will increase the significance of this aim in the future.

**Author Contributions:** Conceptualization, T.M.A. and K.J.S.; writing—original draft preparation, T.M.A. and K.J.S.; writing—review and editing, T.M.A. and K.J.S. All authors have read and agreed to the published version of the manuscript.

**Funding:** This research received no external funding.

**Institutional Review Board Statement:** Not applicable.

**Informed Consent Statement:** Not applicable.

**Data Availability Statement:** Not applicable.

**Conflicts of Interest:** The authors declare no conflict of interest.

## References

1. Yadav, D.; Rangabhashiyam, S.; Verma, P.; Singh, P.; Devi, P.; Kumar, P.; Hussain, C.M.; Gaurav, G.K.; Kumar, K.S. Environmental and Health Impacts of Contaminants of Emerging Concerns: Recent Treatment Challenges and Approaches. *Chemosphere* **2021**, *272*, 129492. [[CrossRef](#)]
2. Starling, M.C.V.M.; Amorim, C.C.; Leão, M.M.D. Occurrence, Control and Fate of Contaminants of Emerging Concern in Environmental Compartments in Brazil. *J. Hazard. Mater.* **2019**, *372*, 17–36. [[CrossRef](#)]
3. Valbonesi, P.; Profita, M.; Vasumini, I.; Fabbri, E. Contaminants of Emerging Concern in Drinking Water: Quality Assessment by Combining Chemical and Biological Analysis. *Sci. Total Environ.* **2021**, *758*, 143624. [[CrossRef](#)]
4. Gaston, L.; Lapworth, D.J.; Stuart, M.; Arnscheidt, J. Prioritization Approaches for Substances of Emerging Concern in Groundwater: A Critical Review. *Environ. Sci. Technol.* **2019**, *53*, 6107–6122. [[CrossRef](#)]
5. Maddela, N.R.; Ramakrishnan, B.; Kakarla, D.; Venkateswarlu, K.; Megharaj, M. Major Contaminants of Emerging Concern in Soils: A Perspective on Potential Health Risks. *RSC Adv.* **2022**, *12*, 12396–12415. [[CrossRef](#)]

6. Samrot, A.V.; Justin, C.; Padmanban, S.; Burman, U. A study on the effect of chemically synthesized magnetite nanoparticles on earthworm: *Eudrilus eugeniae*. *Appl. Nanosci.* **2017**, *7*, 17–23. [[CrossRef](#)]
7. Rajput, V.; Chaplygin, V.; Gorovtsov, A.; Fedorenko, A.; Azarov, A.; Chernikova, N.; Barakhov, A.; Minkina, T.; Maksimov, A.; Mandzhieva, S.; et al. Assessing the Toxicity and Accumulation of Bulk- and Nano-CuO in *Hordeum sativum* L. *Environ. Geochem. Health* **2021**, *43*, 2443–2454. [[CrossRef](#)]
8. Vázquez-Tapia, I.; Salazar-Martínez, T.; Acosta-Castro, M.; Meléndez-Castolo, K.A.; Mahlkecht, J.; Cervantes-Avilés, P.; Capparelli, M.V.; Mora, A. Occurrence of Emerging Organic Contaminants and Endocrine Disruptors in Different Water Compartments in Mexico—A Review. *Chemosphere* **2022**, *308*, 136285. [[CrossRef](#)]
9. Hassan, M.H.; Khan, R.; Andreescu, S. Advances in Electrochemical Detection Methods for Measuring Contaminants of Emerging Concerns. *Electrochem. Sci. Adv.* **2021**, *2*, e2100184. [[CrossRef](#)]
10. Kempahanumakkagari, S.; Deep, A.; Kim, K.-H.; Kumar Kailasa, S.; Yoon, H.-O. Nanomaterial-Based Electrochemical Sensors for Arsenic—A Review. *Biosens. Bioelectron.* **2017**, *95*, 106–116. [[CrossRef](#)]
11. Muscalu, A.M.; Gorecki, T. Comprehensive two-dimensional gas chromatography in environmental analysis. *Trends Anal. Chem.* **2018**, *106*, 225–245. [[CrossRef](#)]
12. Prebihalo, S.; Brockman, A.; Cochran, J.; Dorman, F.L. Determination of emerging contaminants in wastewater utilizing comprehensive two-dimensional gas-chromatography coupled with time-of-flight mass spectrometry. *J. Chromatogr. A* **2015**, *1419*, 109–115. [[CrossRef](#)]
13. Dimpe, K.M.; Nomngongo, P.N. Current sample preparation methodologies for analysis of emerging pollutants in different environmental matrices. *Trends Anal. Chem.* **2016**, *82*, 199–207. [[CrossRef](#)]
14. van Leeuwen, S.P.J.; de Boer, J. Advances in the gas chromatographic determination of persistent organic pollutants in the aquatic environment. *J. Chromatogr. A* **2008**, *1186*, 161–182. [[CrossRef](#)]
15. Santos, F.J.; Galceran, M.T. The application of gas chromatography to environmental analysis. *Trends Anal. Chem.* **2002**, *21*, 672–685. [[CrossRef](#)]
16. He, Q.; Wang, B.; Liang, J.; Liu, J.; Liang, B.; Li, G.; Long, Y.; Zhang, G.; Liu, H. Research on the construction of portable electrochemical sensors for environmental compounds quality monitoring. *Mater. Today Adv.* **2023**, *17*, 100340. [[CrossRef](#)]
17. Buledi, J.A.; Shah, Z.-H.; Mallah, A.; Solangi, A.R. Current Perspective and Developments in Electrochemical Sensors Modified with Nanomaterials for Environmental and Pharmaceutical Analysis. *Curr. Anal. Chem.* **2022**, *18*, 102–115. [[CrossRef](#)]
18. Govindhan, M.; Adhikari, B.-R.; Chen, A. Nanomaterials-Based Electrochemical Detection of Chemical Contaminants. *RSC Adv.* **2014**, *4*, 63741–63760. [[CrossRef](#)]
19. Sivaranjane, R.; Kumar, P.S.; Saravanan, R.; Govarthanan, M. Electrochemical Sensing System for the Analysis of Emerging Contaminants in Aquatic Environment: A Review. *Chemosphere* **2022**, *294*, 133779. [[CrossRef](#)]
20. Kanoun, O.; Lazarević-Pašti, T.; Pašti, I.; Nasraoui, S.; Talbi, M.; Brahem, A.; Adiraju, A.; Sheremet, E.; Rodriguez, R.D.; Ali, M.B.; et al. A Review of Nanocomposite-Modified Electrochemical Sensors for Water Quality Monitoring. *Sensors* **2021**, *21*, 4131. [[CrossRef](#)]
21. Saha, K.; Agasti, S.S.; Kim, C.; Li, X.; Rotello, V.M. Gold Nanoparticles in Chemical and Biological Sensing. *Chem. Rev.* **2012**, *112*, 2739–2779. [[CrossRef](#)]
22. Khanmohammadi, A.; Ghazizadeh, A.J.; Hashemi, P.; Afkhami, A.; Arduini, F.; Bagheri, H. An Overview to Electrochemical Biosensors and Sensors for the Detection of Environmental Contaminants. *J. Iran. Chem. Soc.* **2020**, *17*, 2429–2447. [[CrossRef](#)]
23. Tajik, S.; Beitollahi, H.; Mohammadi, S.Z.; Azimzadeh, M.; Zhang, K.; Van Le, Q.; Yamauchi, Y.; Jang, H.W.; Shokouhimehr, M. Recent Developments in Electrochemical Sensors for Detecting Hydrazine with Different Modified Electrodes. *RSC Adv.* **2020**, *10*, 30481–30498. [[CrossRef](#)]
24. Rana, A.; Baig, N.; Saleh, T.A. Electrochemically Pretreated Carbon Electrodes and Their Electroanalytical Applications—A Review. *J. Electroanal. Chem.* **2019**, *833*, 313–332. [[CrossRef](#)]
25. Sharma, S.; Singh, N.; Tomar, V.; Chandra, R. A Review on Electrochemical Detection of Serotonin Based on Surface Modified Electrodes. *Biosens. Bioelectron.* **2018**, *107*, 76–93. [[CrossRef](#)]
26. Pournara, A.D.; Tarlas, G.D.; Papaefstathiou, G.S.; Manos, M.J. Chemically Modified Electrodes with MOFs for the Determination of Inorganic and Organic Analytes via Voltammetric Techniques: A Critical Review. *Inorg. Chem. Front.* **2019**, *6*, 3440–3455. [[CrossRef](#)]
27. Baibarac, M.; Toulbe, N. Nanostructures Based Detection of Pharmaceuticals and Other Contaminants of Emerging Concern. In *Advanced Nanostructures for Environmental Health*; Baia, L., Pap, Z., Hernadi, K., Baia, M., Eds.; Elsevier: Amsterdam, The Netherlands, 2020; pp. 75–114. [[CrossRef](#)]
28. Salimi, M.; Esrafil, A.; Gholami, M.; Jonidi Jafari, A.; Kalantary, R.R.; Farzadkia, M.; Kermani, M.; Sobhi, H.R. Contaminants of Emerging Concern: A Review of New Approach in AOP Technologies. *Environ. Monit. Assess.* **2017**, *189*, 414. [[CrossRef](#)]
29. Shah, A.I.; Dar, M.U.D.; Bhat, R.A.; Singh, J.P.; Singh, K.; Bhat, S.A. Prospectives and Challenges of Wastewater Treatment Technologies to Combat Contaminants of Emerging Concerns. *Ecol. Eng.* **2020**, *152*, 105882. [[CrossRef](#)]
30. Diamond, J.M.; Latimer, H.A.; Munkittrick, K.R.; Thornton, K.W.; Bartell, S.M.; Kidd, K.A. Prioritizing Contaminants of Emerging Concern for Ecological Screening Assessments. *Environ. Toxicol. Chem.* **2011**, *30*, 2385–2394. [[CrossRef](#)]
31. Rüdél, H.; Körner, W.; Letzel, T.; Neumann, M.; Nödler, K.; Reemtsma, T. Persistent, Mobile and Toxic Substances in the Environment: A Spotlight on Current Research and Regulatory Activities. *Environ. Sci. Eur.* **2020**, *32*, 5. [[CrossRef](#)]

32. Pacheco, C.R.; Hilaire, R.T.; Andrade, G.C.; Mogrovejo-Valdivia, A.; Tanaka, D.A.P. Emerging Contaminants, SARS-CoV-2 and Wastewater Treatment Plants, New Challenges to Confront: A Short Review. *Bioresour. Technol. Rep.* **2021**, *15*, 100731. [[CrossRef](#)]
33. Zhou, S.; Di Paolo, C.; Wu, X.; Shao, Y.; Seiler, T.-B.; Hollert, H. Optimization of Screening-Level Risk Assessment and Priority Selection of Emerging Pollutants—The Case of Pharmaceuticals in European Surface Waters. *Environ. Int.* **2019**, *128*, 1–10. [[CrossRef](#)]
34. Li, W.C. Occurrence, Sources, and Fate of Pharmaceuticals in Aquatic Environment and Soil. *Environ. Pollut.* **2014**, *187*, 193–201. [[CrossRef](#)]
35. Shi, Q.; Xiong, Y.; Kaur, P.; Sy, N.D.; Gan, J. Contaminants of Emerging Concerns in Recycled Water: Fate and Risks in Agroecosystems. *Sci. Total Environ.* **2022**, *814*, 152527. [[CrossRef](#)] [[PubMed](#)]
36. Tang, Y.; Zhong, Y.; Li, H.; Huang, Y.; Guo, X.; Yang, F.; Wu, Y. Contaminants of Emerging Concern in Aquatic Environment: Occurrence, Monitoring, Fate, and Risk Assessment. *Water Environ. Res.* **2020**, *92*, 1811–1817. [[CrossRef](#)]
37. Deere, J.R.; Moore, S.; Ferrey, M.; Jankowski, M.D.; Primus, A.; Convertino, M.; Servadio, J.L.; Phelps, N.B.D.; Hamilton, M.C.; Chenaux-Ibrahim, Y.; et al. Occurrence of Contaminants of Emerging Concern in Aquatic Ecosystems Utilized by Minnesota Tribal Communities. *Sci. Total Environ.* **2020**, *724*, 138057. [[CrossRef](#)]
38. Meador, J.P.; Yeh, A.; Young, G.; Gallagher, E.P. Contaminants of Emerging Concern in a Large Temperate Estuary. *Environ. Pollut.* **2016**, *213*, 254–267. [[CrossRef](#)]
39. Mohapatra, D.P.; Cledón, M.; Brar, S.K.; Surampalli, R.Y. Application of Wastewater and Biosolids in Soil: Occurrence and Fate of Emerging Contaminants. *Water Air Soil Pollut.* **2016**, *227*, 77. [[CrossRef](#)]
40. Ahmed, M.B.; Jahir, M.A.H.; McLaughlan, R.; Nguyen, L.N.; Xu, B.; Nghiem, L.D. Per- and Polyfluoroalkyl Substances in Soil and Sediments: Occurrence, Fate, Remediation and Future Outlook. *Sci. Total Environ.* **2020**, *748*, 141251. [[CrossRef](#)]
41. Shigei, M.; Ahrens, L.; Hazaymeh, A.; Dalahmeh, S.S. Per- and Polyfluoroalkyl Substances in Water and Soil in Wastewater-Irrigated Farmland in Jordan. *Sci. Total Environ.* **2020**, *716*, 137057. [[CrossRef](#)]
42. Balducci, C.; Perilli, M.; Romagnoli, P.; Cecinato, A. New Developments on Emerging Organic Pollutants in the Atmosphere. *Environ. Sci. Pollut. Res.* **2012**, *19*, 1875–1884. [[CrossRef](#)]
43. Salgueiro-González, N.; de Alda, M.J.L.; Muniategui-Lorenzo, S.; Prada-Rodríguez, D.; Barceló, D. Analysis and Occurrence of Endocrine-Disrupting Chemicals in Airborne Particles. *TrAC Trends Anal. Chem.* **2015**, *66*, 45–52. [[CrossRef](#)]
44. Zeng, Y.; Chen, S.; Fan, Y.; Li, Q.; Guan, Y.; Mai, B. Effects of Carbonaceous Materials and Particle Size on Oral and Inhalation Bioaccessibility of PAHs and OPEs in Airborne Particles. *Environ. Sci. Pollut. Res.* **2021**, *28*, 62133–62141. [[CrossRef](#)] [[PubMed](#)]
45. Wang, Y.; Huang, J.; Zhu, F.; Zhou, S. Airborne Microplastics: A Review on the Occurrence, Migration and Risks to Humans. *Bull. Environ. Contam. Toxicol.* **2021**, *107*, 657–664. [[CrossRef](#)]
46. Ageel, H.K.; Harrad, S.; Abdallah, M.A.-E. Occurrence, Human Exposure, and Risk of Microplastics in the Indoor Environment. *Environ. Sci. Process. Impacts* **2022**, *24*, 17–31. [[CrossRef](#)]
47. Bayabil, H.K.; Teshome, F.T.; Li, Y.C. Emerging Contaminants in Soil and Water. *Front. Environ. Sci.* **2022**, *10*, 873499. [[CrossRef](#)]
48. Patel, M.; Kumar, R.; Kishor, K.; Mlsna, T.; Pittman, C.U.; Mohan, D. Pharmaceuticals of Emerging Concern in Aquatic Systems: Chemistry, Occurrence, Effects, and Removal Methods. *Chem. Rev.* **2019**, *119*, 3510–3673. [[CrossRef](#)]
49. Barbosa, M.O.; Moreira, N.F.F.; Ribeiro, A.R.; Pereira, M.F.R.; Silva, A.M.T. Occurrence and Removal of Organic Micropollutants: An Overview of the Watch List of EU Decision 2015/495. *Water Res.* **2016**, *94*, 257–279. [[CrossRef](#)]
50. Michael, I.; Rizzo, L.; McArdell, C.S.; Manai, C.M.; Merlin, C.; Schwartz, T.; Dagot, C.; Fatta-Kassino, D. Urban wastewater treatment plants as hotspots for the release of antibiotics in the environment: A review. *Water Res.* **2013**, *47*, 957–995. [[CrossRef](#)]
51. Gao, X.; Kang, S.; Xiong, R.; Chen, M. Environment-Friendly Removal Methods for Endocrine Disrupting Chemicals. *Sustainability* **2020**, *12*, 7615. [[CrossRef](#)]
52. Diamanti-Kandarakis, E.; Bourguignon, J.-P.; Giudice, L.C.; Hauser, R.; Prins, G.S.; Soto, A.M.; Zoeller, R.T.; Gore, A.C. Endocrine-Disrupting Chemicals: An Endocrine Society Scientific Statement. *Endocr. Rev.* **2009**, *30*, 293–342. [[CrossRef](#)]
53. Furst, A.L.; Hoepker, A.C.; Francis, M.B. Quantifying Hormone Disruptors with an Engineered Bacterial Biosensor. *ACS Cent. Sci.* **2017**, *3*, 110–116. [[CrossRef](#)]
54. Chang, H.-S.; Choo, K.-H.; Lee, B.; Choi, S.-J. The Methods of Identification, Analysis, and Removal of Endocrine Disrupting Compounds (EDCs) in Water. *J. Hazard. Mater.* **2009**, *172*, 1–12. [[CrossRef](#)] [[PubMed](#)]
55. Dallinga, J.W. Decreased Human Semen Quality and Organochlorine Compounds in Blood. *Hum. Reprod.* **2002**, *17*, 1973–1979. [[CrossRef](#)] [[PubMed](#)]
56. Grindler, N.M.; Allsworth, J.E.; Macones, G.A.; Kannan, K.; Roehl, K.A.; Cooper, A.R. Persistent Organic Pollutants and Early Menopause in U.S. Women. *PLoS ONE* **2015**, *10*, e0116057. [[CrossRef](#)] [[PubMed](#)]
57. Smital, T.; Luckenbach, T.; Sauerborn, R.; Hamdoun, A.M.; Vega, R.L.; Epel, D. Emerging Contaminants—Pesticides, PPCPs, Microbial Degradation Products and Natural Substances as Inhibitors of Multixenobiotic Defense in Aquatic Organisms. *Mutat. Res. Fundam. Mol. Mech. Mutagen.* **2004**, *552*, 101–117. [[CrossRef](#)] [[PubMed](#)]
58. Pantelaki, I.; Voutsas, D. Organophosphate Flame Retardants (OPFRs): A Review on Analytical Methods and Occurrence in Wastewater and Aquatic Environment. *Sci. Total Environ.* **2019**, *649*, 247–263. [[CrossRef](#)] [[PubMed](#)]
59. Yang, J.; Zhao, Y.; Li, M.; Du, M.; Li, X.; Li, Y. A Review of a Class of Emerging Contaminants: The Classification, Distribution, Intensity of Consumption, Synthesis Routes, Environmental Effects and Expectation of Pollution Abatement to Organophosphate Flame Retardants (OPFRs). *Int. J. Mol. Sci.* **2019**, *20*, 2874. [[CrossRef](#)]

60. Li, J.; Chen, Z.; Huang, R.; Miao, Z.; Cai, L.; Du, Q. Toxicity Assessment and Histopathological Analysis of Nano-ZnO against Marine Fish (*Mugilogobius chulae*) Embryos. *J. Environ. Sci.* **2018**, *73*, 78–88. [[CrossRef](#)]
61. Sharma, S. Glassy Carbon: A Promising Material for Micro- and Nanomanufacturing. *Materials* **2018**, *11*, 1857. [[CrossRef](#)]
62. Yi, Y.; Weinberg, G.; Prenzel, M.; Greiner, M.; Heumann, S.; Becker, S.; Schlögl, R. Electrochemical Corrosion of a Glassy Carbon Electrode. *Catal. Today* **2017**, *295*, 32–40. [[CrossRef](#)]
63. Abdel-Aziz, A.M.; Hassan, H.H.; Badr, I.H.A. Activated Glassy Carbon Electrode as an Electrochemical Sensing Platform for the Determination of 4-Nitrophenol and Dopamine in Real Samples. *ACS Omega* **2022**, *7*, 34127–34135. [[CrossRef](#)] [[PubMed](#)]
64. Wang, J.; Kirgöz, Ü.A.; Mo, J.-W.; Lu, J.; Kawde, A.N.; Muck, A. Glassy Carbon Paste Electrodes. *Electrochem. Commun.* **2001**, *3*, 203–208. [[CrossRef](#)]
65. Singh, S.; Wang, J.; Cinti, S. Review—An Overview on Recent Progress in Screen-Printed Electroanalytical (Bio)Sensors. *ECS Sens. Plus* **2022**, *1*, 023401. [[CrossRef](#)]
66. Yamanaka, K.; Vestergaard, M.; Tamiya, E. Printable Electrochemical Biosensors: A Focus on Screen-Printed Electrodes and Their Application. *Sensors* **2016**, *16*, 1761. [[CrossRef](#)]
67. Whittingham, M.J.; Hurst, N.J.; Crapnell, R.D.; Ferrari, A.G.-M.; Blanco, E.; Davies, T.J.; Banks, C.E. Electrochemical Improvements Can Be Realized via Shortening the Length of Screen-Printed Electrochemical Platforms. *Anal. Chem.* **2021**, *93*, 16481–16488. [[CrossRef](#)]
68. Hayat, A.; Marty, J. Disposable Screen Printed Electrochemical Sensors: Tools for Environmental Monitoring. *Sensors* **2014**, *14*, 10432–10453. [[CrossRef](#)]
69. Metters, J.P.; Kadara, O.M.; Banks, C.E. New directions in screen-printed electroanalytical sensors: An overview of recent developments. *Analyst* **2011**, *136*, 1067–1076. [[CrossRef](#)]
70. Rodriguez, P.; Koper, M.T.M. Electrocatalysis on Gold. *Phys. Chem. Chem. Phys.* **2014**, *16*, 13583–13594. [[CrossRef](#)]
71. Bollella, P. Porous Gold: A New Frontier for Enzyme-Based Electrodes. *Nanomaterials* **2020**, *10*, 722. [[CrossRef](#)]
72. Xu, X.; Makaraviciute, A.; Pettersson, J.; Zhang, S.-L.; Nyholm, L.; Zhang, Z. Revisiting the Factors Influencing Gold Electrodes Prepared Using Cyclic Voltammetry. *Sens. Actuators B Chem.* **2019**, *283*, 146–153. [[CrossRef](#)]
73. Angnes, L.; Richter, E.M.; Augelli, M.A.; Kume, G.H. Gold Electrodes from Recordable CDs. *Anal. Chem.* **2000**, *72*, 5503–5506. [[CrossRef](#)] [[PubMed](#)]
74. Zeng, A.; Neto, V.F.; Gracio, J.J.; Fan, Q.H. Diamond-like Carbon (DLC) Films as Electrochemical Electrodes. *Diam. Relat. Mater.* **2014**, *43*, 12–22. [[CrossRef](#)]
75. Triroj, N.; Saensak, R.; Porntheeraphat, S.; Paosawatyanong, B.; Amornkitbamrung, V. Diamond-Like Carbon Thin Film Electrodes for Microfluidic Bioelectrochemical Sensing Platforms. *Anal. Chem.* **2020**, *92*, 3650–3657. [[CrossRef](#)]
76. Novoselova, I.A.; Fedorishena, E.N.; Panov, E.V. Electrodes from Diamond and Diamond-like Materials for Electrochemical Applications. *J. Superhard Mater.* **2007**, *29*, 24–39. [[CrossRef](#)]
77. Karimi-Maleh, H.; Karimi, F.; Alizadeh, M.; Sanati, A.L. Electrochemical Sensors, a Bright Future in the Fabrication of Portable Kits in Analytical Systems. *Chem. Rec.* **2020**, *20*, 682–692. [[CrossRef](#)]
78. Bard, A.J.; Faulkner, L.R.; White, H.S. *Electrochemical Methods: Fundamentals and Applications*, 3rd ed.; Wiley: New York, NY, USA, 2022.
79. Compton, R.G.; Banks, C.E. *Understanding Voltammetry*, 2nd ed.; Imperial College Press: London, UK, 2010.
80. Osteryoung, J.G.; Schreiner, M.M. Recent Advances in Pulse Voltammetry. *CRC Crit. Rev. Anal. Chem.* **1988**, *19*, S1–S27. [[CrossRef](#)]
81. Bakker, E.; Telting-Diaz, M. Electrochemical Sensors. *Anal. Chem.* **2002**, *74*, 2781–2800. [[CrossRef](#)]
82. Hart, J.P.; Wring, S.A. Screen-printed voltammetric and amperometric electrochemical sensors for decentralized testing. *Electroanalysis* **1994**, *6*, 617–624. [[CrossRef](#)]
83. Baig, N.; Sajid, M.; Saleh, T.A. Recent trends in nanomaterial-modified electrodes for electroanalytical applications. *Trends Anal. Chem.* **2019**, *111*, 47–61. [[CrossRef](#)]
84. Willner, M.R.; Vikesland, P.J. Nanomaterial Enabled Sensors for Environmental Contaminants. *J. Nanobiotechnol.* **2018**, *16*, 95. [[CrossRef](#)]
85. Lu, Y.; Liang, X.; Niyungeko, C.; Zhou, J.; Xu, J.; Tian, G. A Review of the Identification and Detection of Heavy Metal Ions in the Environment by Voltammetry. *Talanta* **2018**, *178*, 324–338. [[CrossRef](#)]
86. Białas, K.; Moschou, D.; Marken, F.; Estrela, P. Electrochemical Sensors Based on Metal Nanoparticles with Biocatalytic Activity. *Microchim. Acta* **2022**, *189*, 172. [[CrossRef](#)] [[PubMed](#)]
87. Magesa, F.; Wu, Y.; Tian, Y.; Vianney, J.-M.; Buza, J.; He, Q.; Tan, Y. Graphene and Graphene like 2D Graphitic Carbon Nitride: Electrochemical Detection of Food Colorants and Toxic Substances in Environment. *Trends Environ. Anal. Chem.* **2019**, *23*, e00064. [[CrossRef](#)]
88. Li, W.; Geng, X.; Guo, Y.; Rong, J.; Gong, Y.; Wu, L.; Zhang, X.; Li, P.; Xu, J.; Cheng, G.; et al. Reduced Graphene Oxide Electrically Contacted Graphene Sensor for Highly Sensitive Nitric Oxide Detection. *ACS Nano* **2011**, *5*, 6955–6961. [[CrossRef](#)] [[PubMed](#)]
89. Wang, J. Carbon-Nanotube Based Electrochemical Biosensors: A Review. *Electroanalysis* **2005**, *17*, 7–14. [[CrossRef](#)]
90. Kim, S.H. Nanoporous Gold: Preparation and Applications to Catalysis and Sensors. *Curr. Appl. Phys.* **2018**, *18*, 810–818. [[CrossRef](#)]
91. Pandey, B.; Bhattarai, J.K.; Pornsuriyasak, P.; Fujikawa, K.; Catania, R.; Demchenko, A.V.; Stine, K.J. Square-Wave Voltammetry Assays for Glycoproteins on Nanoporous Gold. *J. Electroanal. Chem.* **2014**, *717–718*, 47–60. [[CrossRef](#)]

92. Şeker, E.; Shih, W.-C.; Stine, K.J. Nanoporous Metals by Alloy Corrosion: Bioanalytical and Biomedical Applications. *MRS Bull.* **2018**, *43*, 49–56. [[CrossRef](#)] [[PubMed](#)]
93. Yaghi, O.; Kalmutzki, M.J.; Diercks, C.S. *Introduction to Reticular Chemistry Metal-Organic Frameworks and Covalent Organic Frameworks*; Wiley-VCH: Weinheim, Germany, 2019.
94. Li, J.; Xia, J.; Zhang, F.; Wang, Z.; Liu, Q. An Electrochemical Sensor Based on Copper-Based Metal-Organic Frameworks-Graphene Composites for Determination of Dihydroxybenzene Isomers in Water. *Talanta* **2018**, *181*, 80–86. [[CrossRef](#)]
95. Nagel, S.C.; Bromfield, J.J. Bisphenol A: A Model Endocrine Disrupting Chemical with a New Potential Mechanism of Action. *Endocrinology* **2013**, *154*, 1962–1964. [[CrossRef](#)]
96. Almeida, S.; Raposo, A.; Almeida-González, M.; Carrascosa, C. Bisphenol A: Food Exposure and Impact on Human Health. *Compr. Rev. Food Sci. Food Saf.* **2018**, *6*, 1447–1639. [[CrossRef](#)]
97. Crain, D.A.; Eriksen, M.; Iguchi, T.; Jobling, S.; Laufer, H.; LeBlanc, G.A. An ecological assessment of bisphenol-A: Evidence from comparative biology. *Reprod. Toxicol.* **2007**, *24*, 225–239. [[CrossRef](#)]
98. Jeon, G.W. Bisphenol A leaching from polycarbonate baby bottles into baby food causes potential health issues. *Clin. Exp. Pediatr.* **2022**, *65*, 450–452. [[CrossRef](#)]
99. Wang, F.; Yang, J.; Wu, K. Mesoporous Silica-Based Electrochemical Sensor for Sensitive Determination of Environmental Hormone Bisphenol A. *Anal. Chim. Acta* **2009**, *638*, 23–28. [[CrossRef](#)] [[PubMed](#)]
100. Messaoud, N.B.; Ghica, M.E.; Dridi, C.; Ali, M.A.; Brett, C.M.A. Electrochemical sensor based on a multi-walled carbon nanotube and gold nanoparticle for the sensitive detection of bisphenol A. *Sens. Actuators B* **2017**, *253*, 513–522. [[CrossRef](#)]
101. Jiang, L.; Santiago, I.; Ford, J. A Comparative Study of Fouling-Free Nanodiamond and Nanocarbon Electrochemical Sensors for Sensitive Bisphenol A Detection. *Carbon* **2021**, *174*, 390–395. [[CrossRef](#)]
102. Niu, X.; Yang, W.; Wang, G.; Ren, J.; Guo, H.; Gao, J. A Novel Electrochemical Sensor of Bisphenol A Based on Stacked Graphene Nanofibers/Gold Nanoparticles Composite Modified Glassy Carbon Electrode. *Electrochim. Acta* **2013**, *98*, 167–175. [[CrossRef](#)]
103. Sanko, V.; Şenocak, A.; Tümay, S.O.; Orooji, Y.; Demirbas, E.; Khataee, A. An Electrochemical Sensor for Detection of Trace-Level Endocrine Disruptor Bisphenol A Using Mo<sub>2</sub>Ti<sub>2</sub>AlC<sub>3</sub> MAX Phase/MWCNT Composite Modified Electrode. *Environ. Res.* **2022**, *212*, 113071. [[CrossRef](#)] [[PubMed](#)]
104. Baghayeri, M.; Amiri, A.; Fayazi, M.; Nodehi, M.; Esmaelnia, A. Electrochemical detection of bisphenol a on a MWCNTs/CuFe<sub>2</sub>O<sub>4</sub> nanocomposite modified glassy carbon electrode. *Mater. Chem. Phys.* **2021**, *261*, 124247. [[CrossRef](#)]
105. Zhang, R.; Zhang, Y.; Deng, X.; Sun, S.; Li, Y. A Novel Dual-Signal Electrochemical Sensor for Bisphenol A Determination by Coupling Nanoporous Gold Leaf and Self-Assembled Cyclodextrin. *Electrochim. Acta* **2018**, *271*, 417–424. [[CrossRef](#)]
106. Zhu, W.; Yue, X.; Duan, J.; Zhang, Y.; Zhang, W.; Yu, S.; Wang, Y.; Zhang, D.; Wang, J. Electrochemically Co-Reduced 3D GO-C 60 Nanoassembly as an Efficient Nanocatalyst for Electrochemical Detection of Bisphenol S. *Electrochim. Acta* **2016**, *188*, 85–90. [[CrossRef](#)]
107. Kim, K.S.; Jang, J.-R.; Choe, W.-S.; Yoo, P.J. Electrochemical detection of bisphenol A with high sensitivity and selectivity using recombinant protein-immobilized graphene electrodes. *Biosens. Bioelectron.* **2015**, *71*, 214–221. [[CrossRef](#)] [[PubMed](#)]
108. Ezoji, H.; Rahimnejad, M.; Najafpour-Darzi, G. Advanced sensing platform for electrochemical monitoring of the environmental toxin bisphenol A. *Ecotoxicol. Environ. Saf.* **2020**, *190*, 110088. [[CrossRef](#)]
109. Moraes, F.C.; Silva, T.A.; Cesarino, I.; Machado, S.A.S. Effect of the surface organization with carbon nanotubes on the electrochemical detection of bisphenol A. *Sens. Actuators B* **2013**, *177*, 14–18. [[CrossRef](#)]
110. Goulart, L.A.; de Moraes, F.C.; Mascaro, L.H. Influence of the different carbon nanotubes on the development of electrochemical sensors for bisphenol A. *Mater. Sci. Eng. C* **2016**, *58*, 768–773. [[CrossRef](#)]
111. Yang, J.; Wang, X.; Zhang, D.; Wang, L.; Li, Q.; Zhang, L. Simultaneous determination of endocrine disrupting compounds bisphenol F and bisphenol AF using carboxyl functionalized multi-walled carbon nanotubes modified electrode. *Talanta* **2014**, *130*, 207–212. [[CrossRef](#)]
112. Mo, F.; Xie, J.; Wu, T.; Liu, M.; Zhang, Y.; Yao, S. A sensitive electrochemical sensor for bisphenol A on the basis of the AuPd incorporated carboxylic multi-walled carbon nanotube. *Food Chem.* **2019**, *292*, 253–259. [[CrossRef](#)] [[PubMed](#)]
113. Amenyogbe, E.; Chen, G.; Wang, Z.; Lu, X.; Lin, M.; Lin, A.Y. A Review on Sex Steroid Hormone Estrogen Receptors in Mammals and Fish. *Int. J. Endocrinol.* **2020**, *2020*, 5386193. [[CrossRef](#)]
114. Chang, J.; Zhou, J.; Gao, M.; Zhang, H.; Wang, T. Research Advances in the Analysis of Estrogenic Endocrine Disrupting Compounds in Milk and Dairy Products. *Foods* **2022**, *11*, 3057. [[CrossRef](#)]
115. D’Ascenzo, G.; Di Corcia, A.; Gentili, A.; Mancini, R.; Mastropasqua, R.; Nazzari, M.; Samperi, R. Fate of natural estrogen conjugates in municipal sewage transport and treatment facilities. *Sci. Total Environ.* **2003**, *302*, 199–209. [[CrossRef](#)]
116. Pan, G.; Zhao, G.; Wei, M.; Wang, Y.; Zhao, B. Design of Nanogold Electrochemical Immunosensor for Detection of Four Phenolic Estrogens. *Chem. Phys. Lett.* **2019**, *732*, 136657. [[CrossRef](#)]
117. Raymundo-Pereira, P.A.; Campos, A.M.; Vicentini, F.C.; Janegitz, B.C.; Mendonça, C.D.; Furini, L.N.; Boas, N.V.; Calegaro, M.L.; Constantino, C.J.L.; Machado, S.A.S.; et al. Sensitive Detection of Estriol Hormone in Creek Water Using a Sensor Platform Based on Carbon Black and Silver Nanoparticles. *Talanta* **2017**, *174*, 652–659. [[CrossRef](#)] [[PubMed](#)]
118. Chen, X.; Shi, Z.; Hu, Y.; Xiao, X.; Li, G. A Novel Electrochemical Sensor Based on Fe<sub>3</sub>O<sub>4</sub>-Doped Nanoporous Carbon for Simultaneous Determination of Diethylstilbestrol and 17β-Estradiol in Toner. *Talanta* **2018**, *188*, 81–90. [[CrossRef](#)]

119. Ozcan, A.; Topcuogullari, D. Voltammetric determination of 17 $\beta$ -estradiol by cysteamine self-assembled gold nanoparticle modified fumer silica decorated graphene nanoribbon nanocomposite. *Sens. Actuators B Chem.* **2017**, *250*, 85–90. [[CrossRef](#)]
120. Maskini, M.; Ghica, M.E.; Baker, P.G.L.; Iwuoha, E.I.; Brett, C.M.A. Electrochemical sensor based on multiwalled carbon nanotube/gold nanoparticle modified glassy carbon electrode for detection of estradiol in environmental samples. *Electroanalysis* **2019**, *31*, 1925–1933. [[CrossRef](#)]
121. Ke, H.; Liu, M.; Zhuang, L.; Li, Z.; Fan, L.; Zhao, G. A femtomolar level 17 $\beta$ -estradiol electrochemical aptasensor constructed on hierarchical dendritic gold modified boron-doped diamond electrode. *Electrochim. Acta* **2014**, *137*, 146–153. [[CrossRef](#)]
122. Javaid, S.; Lee, J.; Sofianos, M.V.; Douglas-Moore, Z.; Arrigan, D.W.M.; Silvester, D.S. Zinc Oxide Nanoparticles as Antifouling Materials for the Electrochemical Detection of Methylparaben. *ChemElectroChem* **2021**, *8*, 187–194. [[CrossRef](#)]
123. Musa, A.M.; Kiely, J.; Luxton, R.; Honeychurch, K.C. Recent progress in screen-printed electrochemical sensors and biosensors for the detection of estrogens. *Trends Anal. Chem.* **2021**, *139*, 116254. [[CrossRef](#)]
124. Lu, X.; Sun, J.; Sun, X. Recent advances in biosensors for the detection of estrogens in the environment and food. *Trends Anal. Chem.* **2020**, *127*, 115882. [[CrossRef](#)]
125. Yuan, L.; Zhang, J.; Zhou, P.; Chen, J.; Wang, R.; Wen, T.; Li, Y.; Zhou, X.; Jiang, H. Electrochemical sensor based on molecularly imprinted membranes at platinum nanoparticles-modified electrode for determination of 17 $\beta$ -estradiol. *Biosens. Bioelectron.* **2011**, *29*, 29–33. [[CrossRef](#)] [[PubMed](#)]
126. Zhang, X.; Peng, Y.; Bai, J.; Ning, B.; Sun, S.; Hong, X.; Liu, Y.; Liu, Y.; Gao, Z. A novel electrochemical sensor based on electropolymerized molecularly imprinted polymer and gold nanomaterials amplification for estradiol detection. *Sens. Actuators B Chem.* **2014**, *200*, 69–75. [[CrossRef](#)]
127. Santos, A.M.; Wong, A.; Prado, T.M.; Fava, E.L.; Fatibello-Filho, O.; Sotomayor, M.D.P.T.; Moraes, F.C. Voltammetric determination of ethinylestradiol using screen-printed electrode filled with functionalized graphene, graphene quantum dots and magnetic nanoparticles coated with molecularly imprinted polymers. *Talanta* **2021**, *224*, 121804. [[CrossRef](#)]
128. Zoratti, C.; Moretti, R.; Rebutti, L.; Albergati, I.V.; Di Somma, A.; Decorti, G.; Di Bella, S.; Croce, L.S.; Giuffrè, M. Antibiotics and Liver Cirrhosis: What the Physicians Need to Know. *Antibiotics* **2022**, *11*, 31. [[CrossRef](#)]
129. Yang, Q.; Gao, Y.; Kea, J.; Show, P.L.; Ge, Y.; Liu, Y.; Guo, R.; Chen, J. Antibiotics: An overview on the environmental occurrence, toxicity, degradation, and removal methods. *Bioengineered* **2021**, *12*, 7376–7416. [[CrossRef](#)] [[PubMed](#)]
130. Alagumalai, K.; Shanmugam, R.; Chen, S.-M.; Babulal, S.M.; Periyalagan, A. Novel electrochemical method for detection of cytotoxic Tinidazole in aqueous media. *Process Saf. Environ. Prot.* **2021**, *148*, 992–1005. [[CrossRef](#)]
131. Ensafi, A.A.; Nasr-Esfahani, P.; Rezaei, B. Metronidazole determination with an extremely sensitive and selective electrochemical sensor based on graphene nanoplatelets and molecularly imprinted polymers on graphene quantum dots. *Sens. Actuators B Chem.* **2018**, *270*, 192–199. [[CrossRef](#)]
132. Yue, X.; Li, Z.; Zhao, S. A new electrochemical sensor for simultaneous detection of sulfamethoxazole and trimethoprim antibiotics based on graphene and ZnO nanorods modified glassy carbon electrode. *Microchem. J.* **2020**, *159*, 105440. [[CrossRef](#)]
133. Bhengo, T.; Moyo, M.; Shumba, M.; Okonkwo, O.J. Simultaneous oxidative determination of antibacterial drugs in aqueous solutions using an electrode modified with MWCNTs decorated with Fe<sub>3</sub>O<sub>4</sub> nanoparticles. *New J. Chem.* **2018**, *42*, 5014–5023. [[CrossRef](#)]
134. Alam, A.U.; Qin, Y.; Catalano, M.; Wang, L.; Kim, M.J.; Howlader, M.M.R.; Hu, N.-X.; Deen, M.J. Tailoring MWCNTs and  $\beta$ -Cyclodextrin for Sensitive Detection of Acetaminophen and Estrogen. *ACS Appl. Mater. Interfaces* **2018**, *10*, 21411–21427. [[CrossRef](#)]
135. Alagumalai, K.; Babulal, S.M.; Chen, S.-M.; Shanmugam, R.; Yesuraj, J. Electrochemical evaluation of naproxen through Au@f-CNT/GO nanocomposite in environmental water and biological samples. *J. Ind. Eng. Chem.* **2021**, *104*, 32–42. [[CrossRef](#)]
136. Pollap, A.; Baran, K.; Kuszewska, N.; Kochana, J. Electrochemical sensing of ciprofloxacin and paracetamol in environmental water using titanium sol based sensor. *J. Electroanal. Chem.* **2020**, *878*, 114574. [[CrossRef](#)]
137. Sasal, A.; Tyszczyk-Rotko, K.; Chojecki, M.; Korona, T.; Nosal-Wiercińska, A. Direct Determination of Paracetamol in Environmental Samples Using Screen-printed Carbon/Carbon Nanofibers Sensor—Experimental and Theoretical Studies. *Electroanalysis* **2020**, *32*, 1618–1628. [[CrossRef](#)]
138. Madej, M.; Matoga, D.; Skaźnik, K.; Porada, R.; Baś, B.; Kochana, J. A voltammetric sensor based on mixed proton-electron conducting composite including metal-organic framework JUK-2 for determination of citalopram. *Microchim. Acta* **2021**, *188*, 184. [[CrossRef](#)]
139. Kokulnathan, T.; Kumar, J.V.; Chen, S.-M.; Karthik, R.; Elangovan, A.; Muthuraj, V. One-step sonochemical synthesis of 1D  $\beta$ -stannous tungstate nanorods: An efficient and excellent electrocatalyst for the selective electrochemical detection of antipsychotic drug chlorpromazine. *Ultrason. Sonochem.* **2018**, *44*, 231–239. [[CrossRef](#)] [[PubMed](#)]
140. Maddah, B. Developing a Modified Electrode Based on La<sup>3+</sup>/Co<sub>3</sub>O<sub>4</sub> Nanocubes and Its Usage to Electrochemical Detection of Venlafaxine. *Int. J. Environ. Anal. Chem.* **2020**, *100*, 121–133. [[CrossRef](#)]
141. Wang, W.; Wang, X.; Cheng, N.; Luo, Y.; Lin, Y.; Xu, W.; Du, D. Recent advances in nanomaterials-based electrochemical (bio)sensors for pesticides detection. *Trends Anal. Chem.* **2020**, *132*, 116041. [[CrossRef](#)]
142. Tan, X.; Hu, Q.; Wu, J.; Li, X.; Li, P.; Yu, H.; Li, X.; Lei, F. Electrochemical Sensor Based on Molecularly Imprinted Polymer Reduced Graphene Oxide and Gold Nanoparticles Modified Electrode for Detection of Carbofuran. *Sens. Actuators B Chem.* **2015**, *220*, 216–221. [[CrossRef](#)]

143. Tunesi, M.M.; Kalwar, N.; Abbas, M.W.; Karakus, S.; Soomro, R.A.; Kilislioglu, A.; Abro, M.I.; Hallam, K.R. Functionalised CuO Nanostructures for the Detection of Organophosphorus Pesticides: A Non-Enzymatic Inhibition Approach Coupled with Nano-Scale Electrode Engineering to Improve Electrode Sensitivity. *Sens. Actuators B Chem.* **2018**, *260*, 480–489. [[CrossRef](#)]
144. Lu, X.; Tao, L.; Li, Y.; Huang, H.; Gao, F. A Highly Sensitive Electrochemical Platform Based on the Bimetallic Pd@Au Nanowires Network for Organophosphorus Pesticides Detection. *Sens. Actuators B Chem.* **2019**, *284*, 103–109. [[CrossRef](#)]
145. Fan, L.; Zhao, G.; Shi, H.; Liu, M.; Li, Z. A Highly Selective Electrochemical Impedance Spectroscopy-Based Aptasensor for Sensitive Detection of Acetamiprid. *Biosens. Bioelectron.* **2013**, *43*, 12–18. [[CrossRef](#)] [[PubMed](#)]
146. Malode, S.J.; Shetti, N.P.; Reddy, K.R. Highly Sensitive Electrochemical Assay for Selective Detection of Aminotriazole Based on TiO<sub>2</sub>/Poly(CTAB) Modified Sensor. *Environ. Technol. Innov.* **2021**, *21*, 101222. [[CrossRef](#)]
147. Dong, J.; Hou, J.; Jiang, J.; Ai, S. Innovative Approach for the Electrochemical Detection of Non-Electroactive Organophosphorus Pesticides Using Oxime as Electroactive Probe. *Anal. Chim. Acta* **2015**, *885*, 92–97. [[CrossRef](#)] [[PubMed](#)]
148. Ilager, D.; Malode, S.J.; Kulkarni, R.M.; Shetti, N.P. Electrochemical Sensor Based on Ca-Doped ZnO Nanostructured Carbon Matrix for Algicide Dichlone. *J. Hazard. Mater. Adv.* **2022**, *7*, 100132. [[CrossRef](#)]
149. Gao, Y.; Bian, C.; Ma, H.; Liu, H. Electroactive nanoporous gold driven electrochemical sensor for the simultaneous detection of carbendazim and methyl parathion. *Electrochim. Acta* **2019**, *310*, 78–85. [[CrossRef](#)]
150. Revathi, M.; Kavitha, B.; Vedhi, C.; Senthil Kumar, N. Electrochemical Detection and Quantification of Reactive Red 195 Dyes on Graphene Modified Glassy Carbon Electrode. *J. Environ. Sci. Health Part C* **2019**, *37*, 42–54. [[CrossRef](#)]
151. Clark, R.B.; Dick, J.E. Towards Deployable Electrochemical Sensors for Per- and Polyfluoroalkyl Substances (PFAS). *Chem. Commun.* **2021**, *57*, 8121–8130. [[CrossRef](#)]
152. Faradilla, P.; Setiyanto, H.; Manurung, R.V.; Saraswaty, V. Electrochemical sensor based on screen printed carbon electrode–zinc oxide nano particles/molecularly imprinted-polymer (SPCE–ZnONPs/MIP) for detection of sodium dodecyl sulfate (SDS). *RSC Adv.* **2022**, *12*, 743. [[CrossRef](#)]
153. Bansal, P.; Bhanjana, G.; Prabhakar, N.; Dhau, J.S.; Chaudhary, G.R. Electrochemical sensor based on ZrO<sub>2</sub> NPs/Au electrode sensing layer for monitoring hydrazine and catechol in real water samples. *J. Mol. Liq.* **2017**, *248*, 651–665. [[CrossRef](#)]
154. Malode, S.J.; Prabhu, K.; Pollet, B.G.; Kalanur, S.S.; Shetti, N.P. Preparation and performance of WO<sub>3</sub>/rGO modified carbon sensor for enhanced electrochemical detection of triclosan. *Electrochim. Acta* **2022**, *429*, 141010. [[CrossRef](#)]
155. Lin, M.; Liu, Y.; Chen, X.; Fei, S.; Ni, C.; Fang, Q.; Liu, C.; Cai, Q. Poly(dopamine) coated gold nanocluster functionalized electrochemical immunosensor for brominated flame retardants using multienzyme-labeling carbon hollow nanochains as signal amplifiers. *Biosens. Bioelectron.* **2013**, *45*, 82–88. [[CrossRef](#)] [[PubMed](#)]
156. Chen, H.; Zhang, Z.; Cai, R.; Rao, W.; Long, F. Molecularly imprinted electrochemical sensor based on nickel nanoparticles-graphene nanocomposites modified electrode for determination of tetrabromobisphenol A. *Electrochim. Acta* **2014**, *117*, 385–392. [[CrossRef](#)]
157. Pang, Y.-H.; Huang, Y.-Y.; Li, W.-Y.; Yang, N.-C.; Shen, X.-F. Electrochemical Detection of Three Monohydroxylated Polycyclic Aromatic Hydrocarbons Using Electroreduced Graphene Oxide Modified Screen-printed Electrode. *Electroanalysis* **2020**, *32*, 1459–1467. [[CrossRef](#)]
158. Amin, I.; van den Brekel, H.; Nemani, K.; Batyrev, E.; de Vooy, A.; van der Weijde, H.; Anasori, B.; Shiju, N.R. Ti<sub>3</sub>C<sub>2</sub>T<sub>x</sub> MXene Polymer Composites for Anticorrosion: An Overview and Perspective. *ACS Appl. Mater. Interfaces* **2022**, *14*, 43749–43758. [[CrossRef](#)]

**Disclaimer/Publisher’s Note:** The statements, opinions and data contained in all publications are solely those of the individual author(s) and contributor(s) and not of MDPI and/or the editor(s). MDPI and/or the editor(s) disclaim responsibility for any injury to people or property resulting from any ideas, methods, instructions or products referred to in the content.